POLITECNICO DI TORINO
Repository ISTITUZIONALE

Use of spectroscopic indicators for the monitoring of bromate generation in ozonated wastewater containing variable concentrations of bromide

(Article begins on next page)

03 April 2024

Use of Spectroscopic Indicators for the Monitoring of Bromate Generation in Ozonated Wastewater Containing Variable Concentrations of Bromide

Barbara Ruffino[a,*], Gregory V. Korshin[b], Mariachiara Zanetti[a]

[a]Department of Environment, Land and Infrastructure Engineering, Politecnico di Torino, Torino, Italy

[b]Department of Civil and Environmental Engineering, University of Washington, Seattle, WA, USA

*Corresponding author
Barbara Ruffino
Department of Environment, Land and Infrastructure Engineering
Politecnico di Torino
Corso Duca degli Abruzzi 24, Torino, Italy
Ph. +39.011.0907663
Email: barbara.ruffino@polito.it

Highlights

- BrO_3^- generation and relationships with $\Delta UVA254$ and ΔTF were studied for $Br^- > 1$ mg/L

- Br^- concentrations > 10 mg/L inhibit the generation of BrO_3^-

- Relative reduction of UVA254 and TF of wastewater are good predictors of BrO_3^- generation

- Exponential curves adequately fit the relationships between $\Delta UVA254$ or ΔTF and BrO_3^-

- BrO_3^- generation is strongly correlated with increases of the spectral slope (300-400 nm)

Abstract: Time-resolved monitoring of bromate and other by-products formed into effluents treated with ozone or advanced oxidation processes in wastewater treatment plants (WWTPs) is time-consuming and expensive. This study examined whether concentrations of bromate formed in wastewater after ozonation in the presence of widely varying bromide levels (from ca. 0.7 to 21.2 mg/L) can be quantified based on measurements of changes in optical properties (differential UV absorbance (ΔUVA), spectral slopes, total or regional fluorescence) of the ozonated samples. Batch ozonation was carried out using a secondary effluent produced at a major wastewater treatment plant located in the Metropolitan Seattle Area. The tests involved raw and bromide-spiked samples treated with ozone doses from 0.1 to 1 mg O_3/ mg DOC. Measurements of the absorbance at 254 nm (UVA254), fluorescence and bromate concentrations were performed on the treated samples.

In the ozonated wastewater the concentration of bromate increased approximately linearly, from < 10 ppb to ca. 200 ppb, without showing the lag phase characteristic for lower ozone doses (<0.4 mg O_3/mg DOC) that was observed in previous studies carried out with concentrations of bromide in the range of 0.05 to 0.5 mg/L. The highest bromide concentrations used in this study (>10 mg/L) tended to inhibit the generation of bromate. Relative reduction of UVA254 and total fluorescence (TF) were found to be good predictors of bromate generation. Specifically, exponential curves could adequately fit the non-linear relationships found to exist between the concentrations of bromate and the relative reductions of the UV254 and TF, for any initial bromide concentrations used in this study. Little formation of bromate was found to occur for reduction ranges for UVA254 and TF of 30-40% and 70-80% respectively. Conversely, rapid increases in bromate generation were observed when the decrease of UVA254 or TF exceeded these threshold values.

1. Introduction

Ozonation has been used since the 1970s to meet discharge requirements for coliform and virus inactivation in effluents of wastewater treatment plants (WWTPs) (Rice et al., 1981). In recent years, ozonation of wastewater has gained increasing attention in the context of upgrading WWTPs to include tertiary treatments. This interest is in large extent due to the capacity of ozone to oxidize recalcitrant endocrine disruptors, pharmaceuticals and personal care products (EDC/PPCP), as well as the predominant organic substrate operationally referred to as effluent organic matter (EfOM) (Zimmermann et al., 2011; Zhang et al., 2019). EfOM properties tend to differ from those of dissolved organic matter (DOM) found in natural aquatic systems (Maizel and Remucal, 2017) due to the notable presence in EfOM of soluble microbial products (SMPs) and related biologically produced compounds. Municipal wastewaters also contain multiple EDC/PPCPs and disinfection by-products (Shon et al., 2006, Chen et al., 2017).

The oxidation of EDC/PPCPs by ozone tends to result in the formation of their transformation products that in many, albeit not all cases, have reduced biological response than the parent compounds (Wert et al., 2007; Dodd et al., 2009). In addition to EDC/PPCP oxidation products, ozonation can generate other undesired species (Wu et al., 2019), notably bromate which is a known human carcinogen whose maximum contaminant level (MCL) in drinking water has been set at 10 μg/L in the United States and Europe. Bromate is produced during ozonation through a multistep process involving the oxidation of bromide (Br^-), ensuing generation of hypobromous acid and bromite and their reactions with ozone (von Gunten and Oliveras, 1998; von Gunten, 2003; Fischbacher et al., 2015; Yao et al., 2017; Yang et al., 2019).

Bromide is present in all water sources at concentrations from <10 to >1000 µg/L in fresh waters and approximately 67 mg/L in seawater (Fabbricino and Korshin, 2009; Ikehata et al., 2013; Heeb et al., 2014; Wang et al., 2017). In recent years, the salinization of groundwater in several regions of the world has caused total dissolved solids (TDS) or chloride concentrations to approach or exceed the U.S. EPA's Secondary Maximum Contaminant Levels (MCLs) of 500 mg/L and 250 mg/L, with consequent increases of bromide concentrations up to 10 mg/L (Szczuka et al., 2017). In wastewater, the bromide levels in the treated effluent may be much higher in areas where seawater rather than surface water is used for toilet flushing (Yang et al., 2005; Sun et al., 2009). Yang et al. (2005) used a fresh water nitrified secondary effluent, a saline nitrified secondary effluent, and a saline chemically enhanced primary treatment (CEPT) effluent, with bromide concentrations of 0.96, 22.0 and 31.5 mg/L respectively, to study the formation of trihalomethanes (THMs) and haloacetic acids (HAAs) from the breakpoint chlorination. To pursue the same aim, Sun and coauthors (2009) doped two non-disinfected wastewater samples, with no or low natural bromide (0.14 mg/L), with five bromide concentrations, from zero to 12.8 mg/L. Wastewater effluents associated with produced water from both conventional and unconventional oil and gas extraction activities can be a source of high bromide concentrations (up to 1000 mg/L) because their origin is from highly evaporated paleoseawater (Wilson and VanBriesen, 2012; Ferrar et al., 2013; Warner et al., 2013). These wastewaters are often referred to as brines (Hladik et al., 2014).

Frequent monitoring of the degradation of individual EDC/PPCP and formation of bromate and other toxic by-products is time-consuming and expensive. To address this difficulty, prior research has examined the performance of surrogate parameters such as differential UV absorbance (ΔUVA) and differential total fluorescence (ΔTF) in the monitoring of the quality of ozonated wastewaters (Gerrity et al., 2012). These options have been implemented in practice. For instance,

the California Department of Public Health (CDPH) published in 2014 a revised draft regulation on groundwater replenishment with recycled water; this regulation requires that at least one surrogate indicator be continuously monitored to evaluate the efficiency of advanced oxidation processes (CDPH, 2014).

Several studies have investigated relationships between the change in UV absorbance and/or total fluorescence and the efficiency in removal of micropollutants during ozone-based wastewater treatment (Li et al., 2016 a, b; Liu et al., 2012 a, b, 2015, 2016; Song et al., 2017; Wert et al., 2009) or other advanced oxidation processes (Dickenson et al., 2009; Li et al., 2013). These studies have been performed for lab, pilot and full scale conditions. To the best of our knowledge, only a limited number of prior studies have examined the correlations between changes of the optical properties of wastewater and formation of bromate. Dickenson et al. (2009) had demonstrated that the formation of bromate during ozonation of wastewater effluents is proportional to the relative reduction of UVA254. Chon et al. (2015) investigated the performance of surrogate indicators (i.e., the relative residual UVA254 or electron donating capacity, EDC) in assessing the efficiency of ozonation of wastewater effluents related to changes in DOM, abatement of micropollutants and formation of bromate. Ross et al. (2016) found an empirical correlation between the normalized differential spectra (that is the differential spectra divided by the influent spectrum) at the wavelengths of 250 and 270 nm and bromate formed during ozonation. By using samples of wastewater effluent and surface water, Li et al. (2017) and Wu et al., (2018) demonstrated that measurements of UVA280 and humic-like fluorescence could be used as alternatives or a complementary approach to conventional methods to monitor the formation of bromate. As detailed in Table S1, most of the above-mentioned studies considered samples of wastewater effluent or freshwater containing bromide concentrations of less than 100 µg/L. The samples with

the highest bromide concentrations were used for the study of Li et al. (2017), where the secondary municipal wastewater effluents had bromide concentrations from 200 to 300 µg/L. There is still information concerning the extent of bromate generation and the relative response of spectroscopic parameters, notably UVA254, spectral slopes and TF, when higher bromide concentrations (i.e. > 1 mg/L) were present in the waters subjected to ozonation.

In this study, batch ozonation tests of a secondary wastewater effluent were carried out to determine yields of bromate (that is the relative bromate concentration normalized to initial bromide) at varying ozone doses and bromide concentrations that were varied from < 1 to 20 mg/L. Correlations between the formation of bromate and simultaneous changes of spectroscopic surrogate parameters, for instance the reduction in UVA254, increase of spectral slopes and reduction in TF, were used to assess their potential for efficient bromate control. Excitation emission matrixes (EEM) of ozonated water were also examined with the aim to establish correlations between the generation of bromate and ozonation-induced changes in the fluorescence of EfOM. The outcomes of this study are expected to provide fundamental information needed for the practical application of spectroscopic indicators as feedback signals that can be employed for the a fast and inexpensive control of ozonation processes.

2. Materials and Methods

2.1 Wastewater and chemicals

A sample of secondary municipal wastewater effluent before disinfection was collected from a local WWTP in Seattle (WA, USA). This plant uses high-rate oxygen activated sludge technology without denitrification (Li et al., 2017). The collected wastewater was filtered through a 0.45 μm filter immediately after it was transported to the research laboratory. Selected characteristics of the wastewater are presented in Table 1. The filtered wastewater sample was kept refrigerated at 4 °C and used within one week of sample collection.

Sodium bromide (NaBr, > 99%) used to spike the wastewater and sodium bromate (NaBrO$_3$, > 99%) were purchased from Sigma Aldrich. The ultrapure water (18.2 MΩ,) used in the experiment was produced by a MilliQ system (Millipore, USA).

Table 1. Characteristics of the wastewater effluent used in the ozonation experiments

pH	7.15±0.03
EC (μS/cm)	1540±2
DOC (mg/L)	10 (*)
BOD (mg/L)	29.5 (*)
cBOD (mg/L)	8.83 (*)
UVA254 (cm^{-1})	0.189±0.001
N-NH$_4^+$ (mg/L)	38.2±0.11
N-NO$_3$- (mg/L)	2.35±0.20
Br- (mg/L)	1.03±0.05 (**)
SO$_4$= (mg/L)	55.7±3.0
Cl- (mg/L)	326±4
Alkalinity (mgCaCO$_3$eq/L)	190±5

(*) values provided by the local WWTP.

(**) The concentration of bromide in the raw wastewater (not spiked by sodium bromide) was indicated elsewhere in the paper as 0.69 mg/L. The latter value resulted from the dilution process used for the preparation of the samples employed in the ozonation tests, as described in more detail in the Supplementary Material.

2.2 Ozonation experiments

Ozone was produced with a generator (IN USA AC-2025; Norwood, MA, USA) fed with pure oxygen gas. Ozone stock solution was prepared by sparging an ozone/oxygen gas mixture through a diffuser placed at the bottom of a pre-cleaned glass container filled with MilliQ water and cooled to 0°C. Oxygen flow and voltage settings of the ozone generator were optimized to obtain a 30 mg/L steady state concentration of ozone in the stock solution. The concentration of ozone in the stock solution and in ozonated samples was determined using the standard indigo colorimetric method 4500-O_3 (Bader and Hoigne, 1982). Potassium indigo trisulfonate and all other needed reagents were ACS-grade and purchased from Sigma–Aldrich.

Ozonation batch tests were carried out in 200 mL flasks. Requisite amounts of ozone stock solution were added to a 75 mL wastewater sample to achieve initial ozone concentrations of 0, 1, 2, 3, 5, 7.5 and 10 mg O_3/L. The detailed procedure of sample preparation is described in the Supplementary Material. The above-mentioned ozone concentrations corresponded to specific ozone doses of 0, 0.1, 0.2, 0.3, 0.5, 0.75 and 1 mg O_3/mg dissolved organic carbon (DOC). DOC units were used henceforth as a measure of EfOM concentration and weight ratios of ozone dose vs. EfOM concentration. Ozonation tests were carried out using samples of the wastewater without

any additional bromide (Br concentration = 0.69 mg/L, after dilution) and those spiked with NaBr to obtain final Br- concentrations of 1.72, 2.85, 5.29, 10.8 and 21.2 mg/L.

After a 20-minute contact time, residual ozone was below detection (<1 µg/L) for all specific ozone doses and Br- concentrations. For this reason, no quenching with Na_2SO_3 to stop the reaction was done. The samples were subsequently processed to determine their absorbance, fluorescence, ammonium and nitrate nitrogen and bromate.

2.3 Analytical methods

Absorbance spectra were measured with a PerkinElmer Lambda 18 spectrophotometer and 1 cm quartz cells. Fluorescence spectra were measured using an Aqualog – Horiba fluorescence spectrophotometer. The range of excitation wavelengths was 220 to 450 nm and that of emission was 245 to 827 nm. Fluorescence data were acquired with a 2 nm interval for both excitation and emission wavelengths. Similarly to prior studies (e.g., Anumol et al., 2015 and Li et al., 2017), the EEMs of the samples were automatically corrected for Raman scattering by subtracting the EEM of the water blank from the EEM of any wastewater sample. Inner filter effects were corrected using the instrument's software that utilized applicable absorbance data. Integration of EEMs was carried out according to prior publications (Gerrity et al., 2012; Sgroi et al., 2017a, b) to calculate the total fluorescence (TF) intensities (in arbitrary fluorescence units) for each sample.

Analyses for ammonium and nitrate nitrogen were carried out using an AA3 nitrogen analyzer. Bromide concentrations were determined by means of IC-ICPMS, using a PerkinElmer Series 200 HPLC coupled with a PerkinElmer SCIEX ELAN DRC-e ICP/MS Spectrometer. These analyses were done according to a prior method (Shi and Adams, 2009)

Bromate analysis was performed using an Applied Biosystems 4000 Q Trap liquid chromatography-tandem mass spectrometry system (LC-MS/MS) equipped with a guard column Thermo Scientific Dionex IonPac TM A16 RFIC[TM], 2x50 mm and a chromatographic column Thermo Scientific Dionex IonPac TM AS16 RFIC[TM], 2x250 mm. A binary eluent consisting of acetonitrile at a 0.2 mL/min flow rate (A) and 1 N methylamine in water at 0.05 mL/min flow rate (B) was used. An injection volume of 25 μL was used. The analyte (only bromate) was quantified using the multiple reaction monitoring (MRM) mode.

3. Results and discussion

3.1 Influence of ozonation on absorbance spectra of wastewater samples

In accord with prior research (Rakness, 2005; Wert et al., 2009) the instantaneous ozone demand (IOD) was defined as the difference between the concentration of dissolved ozone at time zero and that found after 30 s of exposure. Relevant measurements showed that for the samples treated with specific ozone doses of 0.2, 0.6 and 1 mg O_3/mg DOC, the ozone that remained in the solution after a 30-second contact time was 0.0146, 1.42 and 3.26 mg/L, respectively, corresponding to IOD values of 2.0, 4.5 and 6.8 mg/L. These IOD values were similar to those reported in prior literature (Wert et al., 2009).

Ozonation did not have an appreciable effect on the oxidation of ammonia (NH_4^+) to nitrate (NO_3^-) and the difference between the concentrations of NH_4^+ and NO_3^-, before and after ozone exposure, were below than the experimental error (2%).

Measurements of the absorbance of ozonated wastewater and calculations of the corresponding differential absorbance spectra, defined as the difference between the absorbance of a sample

treated with ozone and that of the corresponding untreated sample, showed that ozonation caused a monotonic decrease of EfOM absorbance at all wavelengths (Figure 1), as observed in previous research (Chon et al., 2015; Gerrity et al., 2012; Nanaboina and Korshin, 2010).

UVA254 has been used as a surrogate of the aromaticity of NOM and EfOM (Pi et al., 2005; Wert et al., 2009). Figure S1 reports the differential UVA254 as a function of bromide concentration, for the ozone doses (0.1-1 mg O_3/mg DOC) used in this study. In general, the differential UVA254 increased with increasing ozone doses. However, for ozone doses above 0.2-0.3 mg O_3/mg DOC, concentrations of bromide of more than 5 mg/L led to lower differential UVA254 values. This observation was in agreement with the findings of the prior study of Xue and coauthors (2008), where additions of bromide in the range of 0 to 16.7 μM (1.32 mg/L) were found to lead to lower differential UV absorbance values in the range 250-280 nm after chlorination. Xue and coauthors (2008) explained the reduction of differential UVA with increasing bromide levels by suggesting that the UV-absorbing moieties in NOM were attacked by both HOCl and HOBr but HOCl was more active in oxidizing NOM chromophores. In the present study, the reduced differential UVA254 values could likely be due to reactions between ozone and bromide that result in the consumption of ozone in reactions other than those with EfOM and ensuing generation of HOBr and other bromate precursors.

Figure 2a shows the relative changes of UVA254 (defined as $\Delta A/A_0$, where A_0 is the absorbance of the untreated sample for a given Br^- concentration) versus the doses of ozone for each of the bromide concentration used in this study. The data demonstrate that the relative residual UVA254 values changed quasi-linearly for specific ozone doses between 0.1 and 0.5 mg O_3/mg DOC, while for higher specific ozone doses (0.75 and 1 mg O_3/mg DOC) the reduction in UVA254 behaved

asymptotically to reach the value of ca. 50% of the initial value. Thus, increasing bromide concentrations were associated with a reduced degradation of EfOM chromophores. This trend was more evident for specific ozone doses larger than 0.5 mg O_3/mg DOC.

The change in the absorbance at the wavelength of 455 nm has been used to quantify the color removal (Wert et al., 2009). Figure 2b shows that the ozonation-induced changes of color of ozonated wastewater were similar, albeit more prominent than, to those of UVA254. A strong correlation between the removal of color and that of absorbance at 254 nm was observed (Figure 3). This correlation seemed not to depend on the bromide concentration and had a nearly linear trend, following the expression given in (1)

Color depletion = 1,432 · UVA254 depletion + 0.094   (1)   ($R^2 = 0.97$)

Information obtained from the single wavelength absorbance parameters (i.e. 254 nm or 455 nm) can be enhanced through the determination of multi-wavelength spectroscopic indicators, for instance via measurements of the spectral slopes (Helms et al. 2008; Roccaro et al., 2015) of wastewater prior to and after its ozonation. The slopes of the log-transformed absorbance spectra are determined as shown in (2)

$$S_{\lambda_1-\lambda_2} = \left|\frac{dlnA(\lambda)}{d\lambda}\right|_{\lambda_1-\lambda_2}$$ (2)

where lnA(λ) is the natural logarithm of EfOM or NOM absorbance at any specific wavelength, while λ_1 and λ_2 define the range of wavelength in which the spectral slope is calculated. Prior research has shown that the slope of the linear portion of the log-transformed absorbance spectra, e.g. that in the range 300 to 400 nm, tended to be inversely proportional to the average molecular weight of the EfOM or NOM found in the sample (Yan et al., 2014).

Examination of the changes of the spectral slopes (determined for a 300 to 400 nm wavelength range) at varying ozone doses and bromide concentrations (Figure 4) showed two trends. First, similarly to the behavior of UV254 and color, the spectral slope behaved asymptotically for ozone specific doses above 0.5 mg O_3/mg DOC, changing from ca. 0.013 nm^{-1} to above 0.016 nm^{-1}. This is likely to be indicative of the breakdown of EfOM molecules. On the other hand, the inhibiting effect of Br- on the oxidation of organic compounds was associated with lower changes of the spectral slope at increasing bromide concentrations.

3.2 Bromate formation during ozonation of wastewater containing varying bromide concentrations

Figure 5a shows the concentration of bromate in the ozonated samples at specific ozone doses and bromide concentrations. The concentration of bromate increased approximately linearly with the specific ozone dose and ranged from < 10 ppb to ca. 200 ppb. Table 2 provides a compilation of parameters of linear fits between the concentrations of bromate and the specific ozone dose for each bromide concentration. Data presented in Table 2 and Figure 5a show that, while the correlation between the specific ozone dose and bromate generation was nearly perfect for bromide concentration up to ca. 5 mg/L, it deviated from linearity for higher Br- concentrations. In fact, it can be observed that for the specific ozone doses above 0.5 mg O_3/mg DOC, the generation of bromate in the system with a Br$^-$ concentration of 21.2 mg/L largely plateaued. In that system the final concentration of bromate was only in the order of 120 ppb, that is 25% less of the value found, for the same ozone dose, in the system with a Br- concentration of 2.85 mg/L.

Molar bromate yield can be defined as the dimensionless ratio of molar bromate concentrations normalized by the initial bromide concentration (BrO$_3$/Br, mmol L^{-1}/mmol L^{-1}). The trend in molar

bromate yields as a function of the specific ozone dose for each initial bromide concentration is shown in Figure 5b. In the case of un-spiked wastewater with its low bromide concentration, the bromate yield was as high as 10% for the highest dose of ozone. In comparison, bromate yields decreased to below 0.5% for the highest bromide concentrations.

Table 2. Slope and the regression coefficients obtained for the linear fit between the concentrations of bromate and the variation of O_3/DOC ratio

Br- concentration (mg/L)	Slope of the linear fit	R^2
0.693	131.5	0.97
1.72	170.4	1.00
2.85	179.5	0.99
5.29	163.1	0.98
10.8	158.2	0.97
21.2	123.7	0.88

Previous studies (Chon et al., 2015; Soltermann et al., 2016; Li et al., 2017; Wu et al., 2018) have demonstrated that the bromate generation in systems containing EfOM could be described by two phases characterized by their ranges of specific ozone doses. A first phase, for specific ozone doses < 0.25-0.3 mg O_3/mg DOC, was characterized by a negligible bromate formation and a minor effect of the initial bromide concentration. For specific ozone doses > 0.3 mg O_3/mg DOC, the concentrations of bromate increased almost linearly with increasing specific ozone doses (Chon et al., 2015). However, in the study of Chon and coauthors (2015), the concentration of bromide had a limited range of variation (from 39 to 86 μg/L), which did not seem to affect the molar bromate yield. In the present work, the concentrations of bromide were considerably higher than those used in the aforementioned studies (Chon et al., 2015; Soltermann et al., 2016; Li et al., 2017; Wu et

al., 2018) and ranged in a broader interval, from 0.7 to ca. 20 mg/L. Figure 5b presents the experimental data demonstrating that the bromate yield could be linearly correlated with the specific ozone dose for each of the considered bromide concentrations. Consequently, bromate yields were concluded to be affected both by the specific ozone dose and bromide concentration. To describe the trend of bromate yield as a function of the two above-mentioned variables, two relations were proposed. The first had an exponential form (see Eq. 3),

$$BrO_3\left(\frac{O_3}{DOC}, Br\right) = a + b\left(\frac{O_3}{DOC}\right)^n + c(Br)^m \qquad (3)$$

and the second had a third-order polynomial form (see Eq. 4)

$$BrO_3\left(\frac{O_3}{DOC}, Br\right) = p_{00} + p_{10}\left(\frac{O_3}{DOC}\right) + p_{01}(Br) + p_{11}\left(\frac{O_3}{DOC}\right)(Br) + p_{02}(Br)^2 +$$

$$p_{12}\left(\frac{O_3}{DOC}\right)(Br)^2 + p_{03}(Br)^3 \qquad (4)$$

Best fit coefficients, with a 95% confidence bounds, were obtained by using MATLAB software and are reported in the supplementary material section. Fits of the experimental data with the two analytical functions are shown in Figure S2 and S3, respectively. Following the regression coefficient, it was found that the equation in the polynomial form fitted ($R^2 = 0.92$) the experimental data better than the equation in the exponential form ($R^2 = 0.67$).

The observed bromate concentrations and molar bromate yields were also correlated with two of the spectroscopic parameters introduced above, for instance the decrease of UVA254 (Figure 6a-b) and the increase of spectral slopes (Figure 7a-b). Figures 6 and 7 show that the relationships between each of the spectroscopic parameters and the concentration of bromate in the ozonated wastewater was clearly non-linear. The observed non-linearity could be attributed to the complex

phenomena that involve both the organic substances found in the EfOM and bromide into the wastewater subjected to ozonation. Bromide and the fast-reacting moieties of the EfOM (such as hydroxyl-substituted phenolic functionalities) compete for ozone utilization, and, even if the highly-reactive DOM moieties are quickly oxidized, they could retain some of their UV absorbing properties (Chon et al., 2015). Only when the highly-reactive DOM moieties are partially or completely depleted by the ozone attack, the ozone can oxidize bromide to bromate. At the same time, NOM moieties with relatively low reactivity (such as unsubstituted aromatic functionalities), that are much less affected by ozone, continue to contribute to a persistently present residual amount of UVA254 (von Sonntag and von Gunten, 2012). Furthermore, molecular ozone and the hydroxyl radicals, that are formed as a result of ozone decomposition, play different roles in the depletion of the EfOM and in the process of bromate generation (Mao et al., 2018). For this reason, we can argue that the regression between each of the spectroscopic parameters and the concentration of generated bromate was water specific, with a strong dependence on the ozone-reacting characteristics of the EfOM.

Figure 6a demonstrates that, for a given bromide concentration, the formation of bromate during ozonation of the wastewater, was proportional to the relative reduction of UVA254, as previously observed by Dickenson et al. (2009). Significant bromate concentrations were found starting from values of residual UVA254 in the order of 70%. However, for the same value of UVA254 reduction, higher bromide concentrations led to higher bromate yields. This result was in agreement with the findings of Li et al (2017) who noticed that the plots of BrO_3^- vs. UVA254 diverged into two distinct groups of data for effluents taken from a WWTP (with a bromide concentration of 372.5±85.0 µg/L) and for the sample of freshwater (with a bromide concentration of approximately one third, 116.1 µg/L). In the present work bromide concentrations spanned over

more than one order of magnitude, and each bromide concentration generated a curve that could be adequately fitted, with a 95% confidence bounds, by an exponential curve described by Equation (5)

$$[BrO_3\text{-}] = a \cdot e^{b(\text{UVA254 reduction})} \quad (5)$$

with $1.12 < a < 5.44$; $6.61 < b < 10.2$ and $0.96 < R^2 < 0.99$. The "a" parameter, that is the bromate concentration for a null UVA254 reduction, did not show a definite relation with the concentration of bromide. Conversely, the "b" parameter, that describes the rate of bromate concentration increase, was well correlated with the bromide concentration.

The dependence of the relative bromate yields (defined as bromate concentration normalized by the initial bromide concentration, BrO_3/Br) versus the relative residual UVA254 (Figure 6b) showed two regions. In the relative residual UVA254 range of 100-70%, molar bromate yield (BrO_3/Br, mmol L^{-1}/mmol L^{-1} < 0.01) was very small for all bromide concentrations, even though the variation in bromide concentrations spanned over more than one order of magnitude. As discussed above, in this region the limited reduction of UVA254 was due to the small specific ozone dose applied (O_3/DOC ratio < 0.2-0.3). Under these conditions, the ozone was very quickly consumed, with almost no ozone residual concentration available for bromate formation. Conversely, in the relative residual UVA254 range of 70-40%, the bromate yield appears to be related to the abatement of the relative residual UVA254, especially for bromide concentrations below 5 mg/L. Residual UVA254 values in the order of 70-40% were observed for specific ozone doses from 0.2-0.3 to 1.0 mg O_3/mg DOC. In this range of O_3/DOC ratios, the observed trend of bromate formation was in good agreement with the findings of Chon and coauthors (2015) that

attributed the formation of bromate by the combined action of ozone and hydroxyl radicals to the higher ozone lifetime due to the partially destroyed electron donating DOM moieties.

Figure 7a shows that increases of the spectral slope caused by the ozonation of EfOM were always correlated with the concurrently increasing bromate concentrations but these correlations depended on the initial concentration of bromide. Figure 7b relates the relative bromate normalized to bromide (BrO_3/Br) to the spectral slopes determined for the wavelength range from 300 to 400 nm. It could be observed a trend similar to that found for UVA254 reduction, with two distinct behaviors. For spectral slopes from 0.013 nm^{-1} to 0.017 nm^{-1}, molar bromate yield showed approximately constant values in the order of 0.01 or less. Conversely, for spectral slopes of more than 0.017 nm^{-1}, this spectroscopic parameter seemed to be moderately well correlated with the molar bromate yield.

3.3 Relation between fluorescence parameters and bromate generation

Representative fluorescence EEMs of the untreated raw sample (Br = 0.693 mg/L) and of the raw samples treated with 0.1 and 0.5 mg O_3/mg DOC are shown in Figure S4a, S4b and S4c, respectively. The data shown in Figure S4a demonstrate the presence of four major characteristic structures, the nature of which was attributed in accord with the findings of prior studies (Li et al., 2013; 2016a; Barsotti et al., 2016; Chen et al, 2017) and maxima are listed in Table 3.

Table 3. Area of maximum intensity for the fluorescence acquisition of the raw wastewater sample

Structure	EM (nm)	EX (nm)	Nature
I	330-360	220-230	Protein-like species
II	350-450	240	Fulvic-like species
III	345	280	Protein-like species
IV	430	330	Humic-like species

Properties of the four structures listed in Table 3 differed significantly from each other. The first revealed a zone at high intensity that extended between the EX range of 220-230 nm and the EM range of 330-360 nm. Due to its location, this structure indicated the presence of protein-like species. However, by analyzing this EEM structure with the peak-picking method (Sgroi et al., 2017 a, b), it was not possible to locate a definite peak of intensity in emission but only an area of maximum intensity with an amplitude of approximately 30 nm. A similar consideration can be done for structure II, that was indicative of the presence of fulvic-like species. The maximum intensity covered an area of 100 nm around the EX wavelength of 240 nm. Structures III and IV were instead more defined. For these structures, it was possible to identify an almost unique peak in both excitation and emission modes. The location of structure III, like structure I, was indicative of the presence of protein-like species; conversely, structure IV was indicative of the presence of humic-like species.

Ozonation caused a pronounced decrease of the fluorescence intensity of the treated wastewater. Figures S4b and S4c show this effect on the raw wastewater exposed to 0.1 and 0.5 mg O_3/mg DOC respectively. Figure S4c shows that following an ozonation with a 0.5 mg O_3/mg DOC specific dose, it was no longer possible to identify the structures related to the presence of protein-

like species. In contrast, the structures associated with fulvic-like and humic-like fluorophores were still discernible. Ozonation caused their intensity to decrease and position of the maximum intensity to shift towards higher wavelengths. The peak of structure IV (Table 3) before ozonation was located at (EX 330 nm, EM 430 nm, see Figure S4a) and after ozonation its position was at the excitation and emission wavelengths of 345 nm and 445 nm, respectively (see Figure S4c). These observations, that are consistent with those reported in prior research (Li et al., 2013), indicated that fulvic-like and humic-like compounds in EfOM are comparatively more resistant to oxidation by ozone and HO* radicals than protein-like/SMPs species.

TF integration was performed by summing all the intensity values on the rows and the columns of the EEM, that is by integrating the volume under the whole EEM surface as in (Sgroi et al., 2017 a, b). For discrete EEM data, the parameter TF can be determined as in Equation (6)

$$ TF = \sum_{ex} \sum_{em} I(\lambda_{ex} \lambda_{em}) \Delta\lambda_{ex} \Delta\lambda_{em} \quad (6) $$

where $\Delta\lambda_{ex}$ is the excitation wavelength interval (taken as 2 nm), $\Delta\lambda_{em}$ is the emission wavelength interval (taken as 2 nm), and $I(\lambda_{ex}\lambda_{em})$ is the fluorescence intensity of each excitation–emission wavelength pair.

Figure 8 shows the reduction of TF as a function of the specific dose of ozone. As in the case of UVA_{254} and color, the reduction of TF plateaus for specific ozone doses > 0.5 mg O_3/mg DOC. The maximum reduction of TF was observed for the sample not spiked with Br-, while higher concentrations of bromide decreased the extent of ozone effects on EfOM fluorophores.

The fluorescence data were processed to determine their correlations with the generation of bromate. Figure S5 shows the relationships of the generation of bromate with the reduction in TF,

while Figure 9 presents the normalized (molar) bromate yields as a function of the relative residual TF. Figure S5 shows a trend for bromate generation similar to that observed for the correlation with UVA254 reduction (see Figure 6a). Even in this case the relation between bromate concentration and total fluorescence reduction could be described, with a 95% confidence bounds, by an exponential curve, as in Equation (7)

$$[BrO_3\text{-}] = a \cdot e^{b(Ftot\ reduction)} \qquad (7)$$

with $0.47 < a < 3.74$; $4.41 < b < 6.16$ and $0.92 < R^2 < 0.99$, depending on the initial bromide concentration. Similarly to the relation found to exist between the UVA254 parameters and bromate generation, also in this case the "a" parameter, that is the bromate concentration for a null TF reduction, did not show a definite relation with the concentration of bromide. Conversely, the "b" parameter, that describes the rate of bromate concentration increase, was quite well correlated with the bromide concentration.

In this case, significant bromate concentrations were observed for residual TF in the order of 40%.

Similarly to the trends shown in Figures 6b and 7b, Figure 9 shows the presence of two distinct regions. Low molar bromate yields (< 0.01) could be observed for residual TF up to ca. 30%, followed by a sharp increase of bromate yield for more pronounced changes of TF. In the region with the highest residual TF (80-30%), ozone was rapidly consumed by substances responsible ~~of~~ for fluorescence and little residual ozone is left for reaction with Br-. Conversely, in the second phase, most of the substances responsible of fluorescence had been consumed and a higher ozone dose was available for oxidation of bromide to bromate. This trend was in agreement with the observations of Li and coauthors (2017).

4. Conclusions

This study examined the correlations between changes of optical properties of wastewater treated with ozone and bromate generation in the presence of widely varying initial bromide concentrations, that is in the range from ca. 0.7 to 21.2 mg/L. The major conclusions made based on the reported resulted can be presented as follows.

- The intensity of differential UVA254 increased with increasing ozone doses. However, the compresence of ozone doses above 0.2-0.3 mg O_3/mg DOC and bromide concentrations above 5 mg/L were associated with somewhat lower differential UVA254 values. This is likely to be caused by the occurrence of reactions between ozone and bromide that decreased the extent of reactions between ozone and EfOM and, at the same time, resulted in the generation of HOBr and other bromate precursors.

- For specific doses of ozone from 0.1 to 1 mg O_3/mg DOC, the concentration of bromate increased approximately linearly, from below 10 ppb to ca. 200 ppb, without a lag phase in the correspondence of lower ozone doses (<0.4 mg O_3/mg DOC). Higher bromide concentrations (> 10 mg/L) seemed to inhibit the generation of bromate.

- Relative reduction in UVA254 and TF demonstrated to be good predictors of bromate generation for the entire range of examined bromide concentrations. Specifically, an exponential fitting, $[BrO_3^-] = a \cdot e^{b(UVA254 \text{ or } TF \text{ reduction})}$, proved to adequately fit ($0.92 < R^2 < 0.99$) the non-linear relationships between the concentration of bromate and the relative reduction of the two spectroscopic parameters. The "b" parameter in the model, that describes the rate of bromate concentration increase, was strongly dependent and positively correlated with the initial bromide concentration. It was consistently

observed for the same value of UVA254 or TF reduction, higher initial bromide concentration led to higher bromate generation.

- When the generation of bromate was described based on the relative bromate yields (BrO_3/Br molar ratios), two distinct regions were observed. Molar bromate yields of less than 0.01 were found for residual UVA254 and TF above 70% and 30% respectively. A subsequent sharp increase in the molar bromate yield (from 0.01 to 0.1, depending on the bromide concentration) was observed for more pronounced changes of UVA 254 or TF.

- The generation of bromate was positively correlated with the increase of spectral slopes (300-400 nm), but more observations are necessary to identify a robust correlation between the two parameters. When the normalized bromate yields were plotted vs. the spectral slopes, in the range 0.013 - 0.017 nm^{-1}, they showed approximately constant values in the order of 0.01. Conversely, for spectral slopes of more than 0.017 nm^{-1}, this spectroscopic parameter seemed to be moderately well correlated with the molar bromate yield.

- The results of this study demonstrate that several spectroscopic parameters, notably changes of UV254, spectral slope and TF, can provide a feedback signal for a real-time estimation of bromate generation in wastewater ozonation processes.

Acknowledgements

T.R. Young, from the Department of Civil and Environmental Engineering, University of Washington, Seattle (WA, USA), for fruitful discussions and continuous support in the experimental activities.

References

Anumol, T., Sgroi, M., Park, M., Roccaro, P., Snyder, S.A., 2015. Predicting trace organic compound breakthrough in granular activated carbon using fluorescence and UV absorbance as surrogates. Water Res. 76, 76-87.

Bader, H., Hoigne, J., 1982. Determination of ozone in water by the indigo method; a submitted standard method. Ozone: Sci. Eng. 4 (4), 169–176.

Barsotti, F., Ghigo, G., Vione, D., 2016. Computational assessment of the fluorescence emission of phenol oligomers: a possible insight into the fluorescence properties of humic-like substances (HULIS). J. Photochem. Photobiol. a-Chem. 315, 87-93.

Chen, Z., Li, M., Wen, Q., Ren, N., 2017. Evolution of molecular weight and fluorescence of effluent organic matter (EfOM) during oxidation processes revealed by advanced spectrographic and chromatographic tools, Water Res. 124, 566-575 DOI: 10.1016/j.watres.2017.08.006

Chon, K., Salhi, E., von Gunten, U., 2015. Combination of UV absorbance and electron donating capacity to assess degradation of micropollutants and formation of bromate during ozonation of wastewater effluents. Water Res. 81, 388-397.

CDPH, 2014. CDPH Draft Regulations: Groundwater Replenishment with Recycled Water. CDPH, Sacramento, CA, USA.

Dickenson, E.R., Drewes, J.E., Sedlak, D.L., Wert, E.C., Snyder, S.A., 2009. Applying surrogates and indicators to assess removal efficiency of trace organic chemicals during chemical oxidation of wastewater. Environ. Sci. Technol. 43 (16) 6242–6247.

Dodd, M.C., Kohler, H.P.E., von Gunten, U., 2009. Oxidation of antibacterial compounds by ozone and hydroxyl radical: elimination of biological activity during aqueous ozonation processes. Environ. Sci. Technol. 43 (7), 2498-2504.

Fabbricino, M., Korshin G.V., 2009. Modelling disinfection by-products formation in bromide-containing waters. J. Hazard. Mater. 168, 782-786.

Ferrar, K.J., Michanowicz, D.R., Christen, C.L., Mulcahy, N., Malone, S.L., Sharma, R.K., 2013. Assessment of effluent contaminants from three facilities discharging Marcellus Shale wastewater to surface water in Pennsylvania. Environ. Sci. Technol. 47, 3472–3481.

Fischbacher, A., Löppenberg, K., von Sonntag, C., Schmidt T.C., 2015. A new reaction pathway for bromite to bromate in the ozonation of bromide. Environ. Sci. Technol. 49 (19), 11714-11720.

Gerrity, D., Gamage, S., Jones, D., Korshin, G.V., Lee, Y., Pisarenko, A., Trenholm, R.A., von Gunten, U., Wert, E.C., Snyder, S.A., 2012. Development of surrogate correlation models to predict trace organic contaminant oxidation and microbial inactivation during ozonation. Water Res. 46, 6257-6272.

Hladik, M.L., Focazio, M.J., Engle, M., 2014. Discharges of produced waters from oil and gas extraction via wastewater treatment plants are sources of disinfection by-products to receiving streams. Sci. Total Environ. 466–467, 1085–1093.

Heeb, M.B., Criquet, J., Zimmermann-Steffens, S.G, von Gunten, U., 2014. Oxidative treatment of bromide-containing waters: Formation of bromine and its reactions with inorganic and organic compounds - A critical review. Water Res. 48, 15-42.

Helms, J.R., Stubbins, A., Ritchhie, J.D., Minor, E.C., Kieber, D.J., Mopper, K., 2008. Absorption spectral slopes and slope ratios as indicators of molecular weight, source, and photobleaching of chromophoric dissolved organic matter. Limnol. Oceanogr. 53 (3), 955-969.

Ikehata, K., Wang, L., Nessl, M.B., Komor, A.T., Cooper, W.J., McVicker, R.R., 2013. Effect of Ammonia and Chloramine Pretreatment during the Ozonation of a Colored Groundwater with Elevated Bromide. Ozone: Sci. Eng. 35, 438–447.

Li, W.T, Xu, Z.X, Li, A.M, Wu, W., Zhou, Q., Wang, J.N., 2013. HPLC/HPSEC-FLD with multi-excitation/emission scan for EEM interpretation and dissolved organic matter analysis. Water Res. 47, 1246-1256.

Li, W.T., Jin, J., Li, Q., Wu, C.F., Lu, H., Zhou, Q., Li, A.M., 2016a. Developing LED UV fluorescence sensors for online monitoring DOM and predicting DBPs formation potential during water treatment. Water Res. 93, 1-9.

Li, W., Nanaboina, V., Chen, F., Korshin, G.V., 2016b. Removal of polycyclic synthetic musks and antineoplastic drugs in ozonated wastewater: Quantitation based on the data of differential spectroscopy. J. Hazard. Mater. 304, 242-250.

Li, W.T., Cao, M.J., Young, T., Ruffino, B., Dodd, M., Li, A.M., Korshin, G., 2017. Application of UV absorbance and fluorescence indicators to assess the formation of biodegradable dissolved organic carbon and bromate during ozonation. Water Res. 111, 154-162.

Liu, C., Nanaboina, V. and Korshin, G.V., 2012a. Spectroscopic study of the degradation of antibiotics and the generation of representative EfOM oxidation products in ozonated wastewater. Chemosphere 86 (8), 774-782.

Liu, C., Nanaboina, V., Korshin, G.V. and Jiang, W., 2012b. Spectroscopic study of degradation products of ciprofloxacin, norfloxacin and lomefloxacin formed in ozonated wastewater. Water Res. 46, 5235-5246.

Liu, C., Tang, X., Kim, J. and Korshin, G.V., 2015. Formation of aldehydes and carboxylic acids in ozonated surface water and wastewater: A clear relationship with fluorescence changes. Chemosphere 125, 182-190.

Liu, C., Li, P., Tang, X., Korshin, G.V., 2016. Ozonation effects on emerging micropollutants and effluent organic matter in wastewater: characterization using changes of three-dimensional HP-SEC and EEM fluorescence data. Environ. Sci. Pollut. Res. 23, 20567–20579.

Maizel, A.C., Remucal, C.K., 2017. The effect of advanced secondary municipal wastewater treatment on the molecular composition of dissolved organic matter. Water Res. 122, 42-52.

Mao, Y., Guo, D., Yao, W., Wang, X., Hongwei Yang, H., Xie, Y.F., Komarneni, S., Yu, G., Wang, Y., 2018. Effects of conventional ozonation and electro-peroxone pretreatment of surface water on disinfection by-product formation during subsequent chlorination. Water Res. 130, 322-332.

Nanaboina, V., Korshin, G.V., 2010. Evolution of Absorbance Spectra of Ozonated Wastewater and Its Relationship with the Degradation of Trace-Level Organic Species. Environ. Sci. Technol. 44 (16), 6130-6137.

Pi, Y.; Schumacher, J.; Jekel, M., 2005. Decomposition of aqueous ozone in the presence of aromatic organic solutes. Water Res. 39, 83–88.

Rakness, K.L., 2005. Ozone in Drinking Water Treatment, Process Design, Operation and Optimization. AWWA: Denver, Colorado, ISBN 978-1625760746

Rice, R.G., Evison, L.M., Robson, C.M., 1981. Ozone disinfection of municipal wastewater—current state-of-the-art. Ozone: Sci. Eng. 3 (4), 239–272.

Roccaro P., Yan M., Korshin G.V., 2015. Use of log-transformed absorbance spectra for online monitoring of the reactivity of natural organic matter. Water Res. 84, 136-143.

Ross, P.S., van der Helm, A.W.C., van den Broeked, J., Rietveld, L.C., 2016. On-line monitoring of ozonation through estimation of Ct value, bromate and AOC formation with UV/Vis spectrometry. Anal. Methods 8, 3148-3155.

Sgroi M., Roccaro P., Korshin G.V., Vagliasindi F.G.A., 2017a. Monitoring the Behavior of Emerging Contaminants in Wastewater-Impacted Rivers Based on the Use of Fluorescence Excitation Emission Matrixes (EEM). Environ. Sci. Technol. 51, 4306-4316.

Sgroi, M., Roccaro, P., Korshin, G.V., Greco, V., Sciuto, S., Anumol, T., Snyder, S.A., Vagliasindi, F.G.A., 2017b. Use of fluorescence EEM to monitor the removal of emerging contaminants in full scale wastewater treatment plants. J. Hazard. Mater. 323, 367−376.

Shi, H., Adams, C., 2009. Rapid IC-ICP/MS method for simultaneous analysis of iodoacetic acids, bromoacetic acids, bromate, and other related halogenated compounds in water. Talanta 79 (2), 523-527.

Shon, H.K., Vigneswaran, S., Snyder, S.A., 2006. Effluent organic matter (EfOM) in wastewater: constituents, effects, and treatment. Crit. Rev. Environ. Sci. Technol. 36, 327–374.

Soltermann, F., Abegglen, C., Gotz, C., von Gunten, U., 2016. Bromide sources and loads in Swiss surface waters and their relevance for bromate formation during wastewater ozonation. Environ. Sci. Technol. 50 (18), 9825-9834.

Song, Y., Breider, F., Ma, J., von Gunten, U., 2017. Nitrate formation during ozonation as a surrogate parameter for abatement of micropollutants and the N-nitrosodimethylamine (NDMA) formation potential. Water Res. 122, 246–257.

Sun, Y.X., Wu, Q.Y., Hu, H.Y., Tian, J., 2009. Effect of bromide on the formation of disinfection by-products during wastewater chlorination. Water Res. 43, 2391-2398.

Szczuka, A., Parker, K.M., Harvey, C., Hayes, E., Vengosh, A., Mitch, W.A., 2017. Regulated and unregulated halogenated disinfection byproduct formation from chlorination of saline groundwater. Water Res. 122, 633-644. doi: 10.1016/j.watres.2017.06.028

von Sonntag, C., von Gunten, U., 2012. Chemistry of Ozone in Water and Wastewater Treatment from Basic Principles to Applications. IWA Publishing, London, UK.

von Gunten, U., 2003. Ozonation of drinking water: part II. Disinfection and by-product formation in presence of bromide, iodide or chlorine. Water Res. 37, 1469–1487.

von Gunten, U., Oliveras, Y., 1998. Advanced oxidation of bromide-containing waters: bromate formation mechanisms. Environ. Sci. Technol. 32 (1), 63–70.

Wang, Y., Small, M.J., VanBriesen, J.M., 2017. Assessing the Risk Associated with Increasing Bromide in Drinking Water Sources in the Monongahela River, Pennsylvania. ASCE J. Environ. Eng. 143 (3), 04016089.

Warner, N.R., Christie, C.A., Jackson, R.B., Vengosh, A., 2013. Impacts of Shale Gas Wastewater Disposal on Water Quality in Western Pennsylvania. Environ. Sci. Technol. 47, 11849−11857.

Wert, E.C., Rosario-Ortiz, F.L., Drury, D.D., Snyder, S.A., 2007. Formation of oxidation byproducts from ozonation of wastewater. Water Res. 41, 1481-1490.

Wert, E.C., Rosario-Ortiz, F.L., Snyder, S.A., 2009. Using ultraviolet absorbance and color to assess pharmaceutical oxidation during ozonation of wastewater. Environ. Sci. Technol. 43 (13), 4858-4863.

Wilson, J.M., VanBriesen, J.M., 2012. Oil and gas produced water management and surface drinking water sources in Pennsylvania. Environ Pract. 14, 301–307.

Wu, J., Cheng, S., Cai, M.H., Wu, Y.P., Li, Y., Wu, J.C., Li, A.M., Li, W.T., 2018. Applying UV absorbance and fluorescence indices to estimate inactivation of bacteria and formation of bromate during ozonation of water and wastewater effluent. Water Res. 145, 354-364.

Wu, Q.Y., Zhou, Y.T., Li, W., Zhang, X., Du, Y., Hu, H.Y., 2019. Underestimated risk from ozonation of wastewater containing bromide: Both organic byproducts and bromate contributed to the toxicity increase. Water Res. 162, 43-52.

Xue, S., Zhao, Q.L., Wei, L.L., Jia T., 2008. Effect of bromide ion on isolated fractions of dissolved organic matter in secondary effluent during chlorination. J. Hazard. Mater. 157, 25–33.

Yan, M., Korshin, G.V., Chang, H.S., 2014. Examination of disinfection by-products (DBPs) formation in source waters: a study using log-transformed differential spectra. Water Res. 50, 179-188.

Yang, X., Shang, C., Huang J.C., 2005. DBP formation in breakpoint chlorination of wastewater. Water Res. 39, 4755–4767.

Yang, J., Dong, Z., Jiang, C., Wang, C., Liu, H., 2019. An overview of bromate formation in chemical oxidation processes: Occurrence, mechanism, influencing factors, risk assessment, and control strategies. Chemosphere, 237, 124521.

Yao, W., Qu, Q., Gunten, U., Chen, C., Yu, G., Wang, Y., 2017. Comparison of methylisoborneol and geosmin abatement in surface water by conventional ozonation and an electro-peroxone process. Water Res. 108, 373–382.

Zhang, Y., An, Y., Liu, C., Wang, Y., Song, Z., Li, Y., Meng, W., Qi, F., Xu, B., Croue, J.P., Yuan, D., Ikhlaq, A., 2019. Catalytic ozonation of emerging pollutant and reduction of toxic by-products in secondary effluent matrix and effluent organic matter reaction activity. Water Res. 166, 115026.

Zimmermann, S.G., Wittenwiler, M., Hollender, J., Krauss, M., Ort, C., Siegrist, H., von Gunten, U., 2011. Kinetic assessment and modeling of an ozonation step for full-scale municipal wastewater treatment: micropollutant oxidation, byproduct formation and disinfection. Water Res. 45, 605-617.
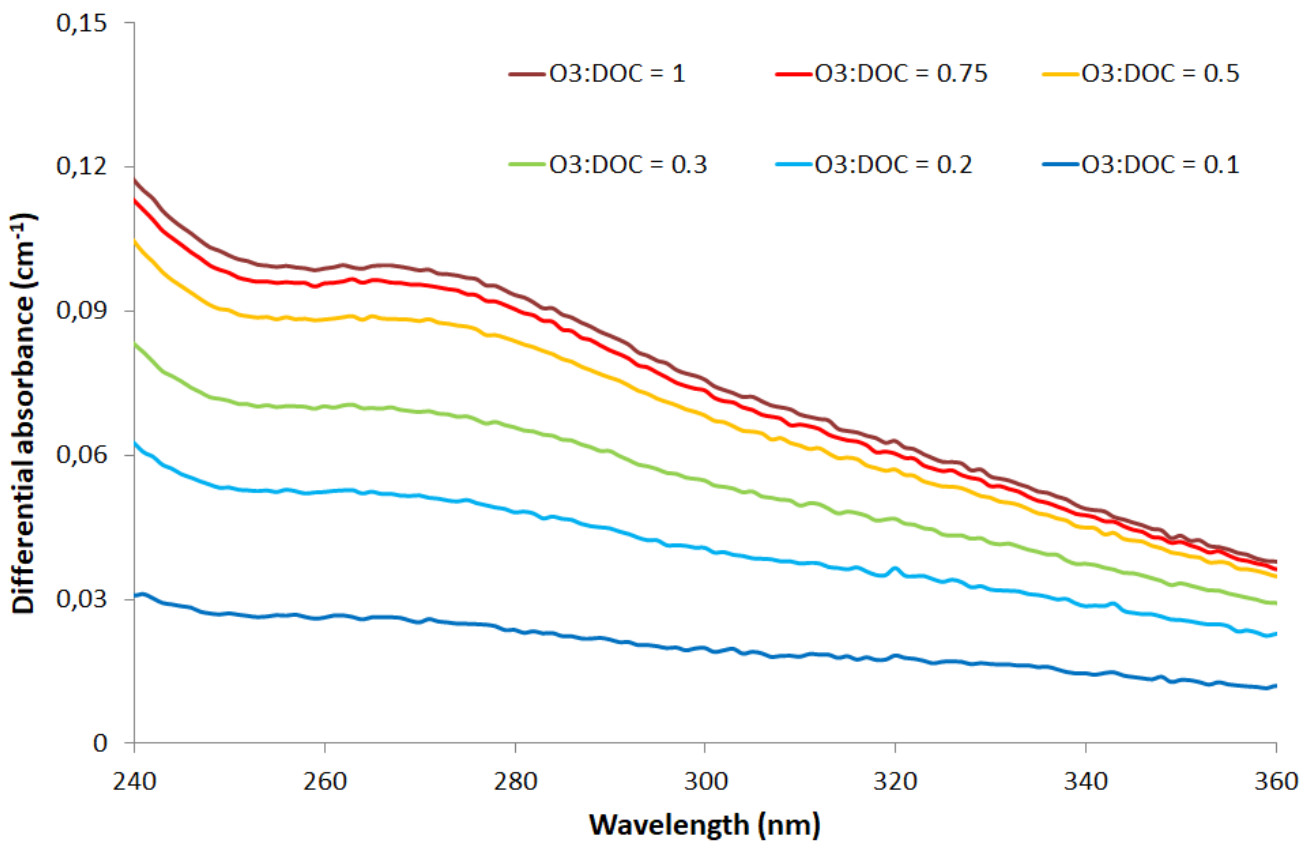
Figure 1. Changes of the differential absorbance spectra (DAS) of ozonated wastewater as a function of ozone doses (0.1 – 1 mg O_3/ mg DOC).

(a)
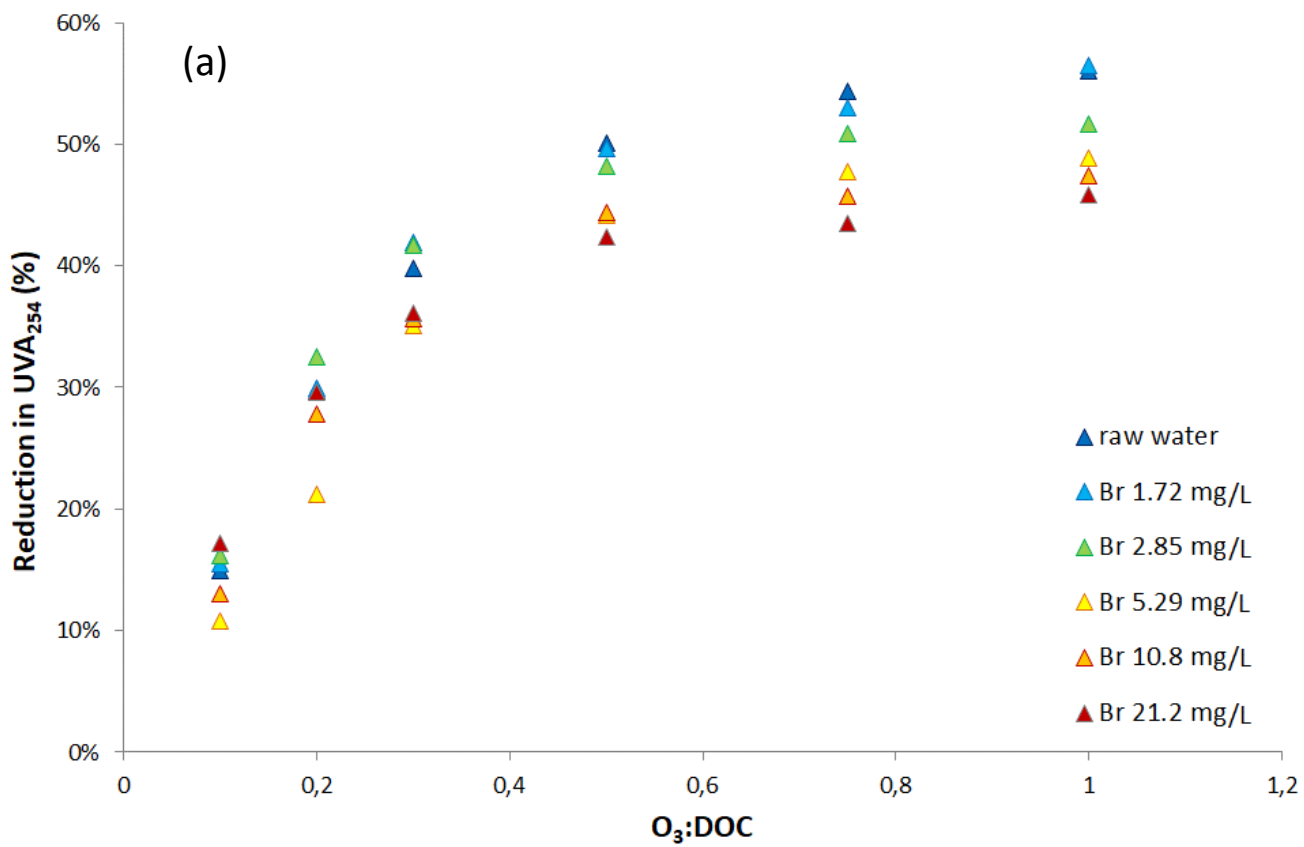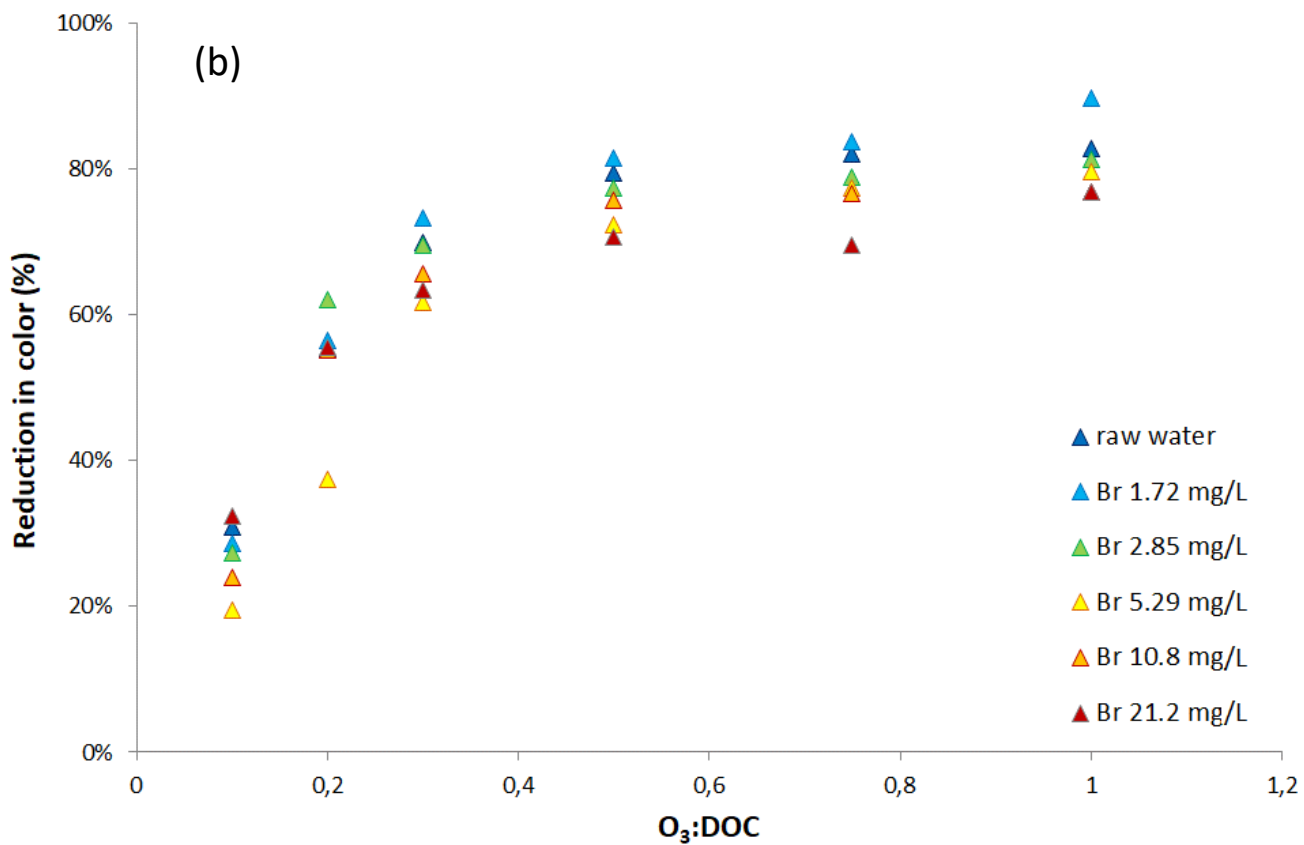
Figure 2. Relative reduction of UVA$_{254}$ (a) and color (b) of ozonated wastewater as a function of the specific ozone dose (0.1 – 1 mg O$_3$/ mg DOC range) and bromide concentration (0.69 – 21.2 mg/L range).
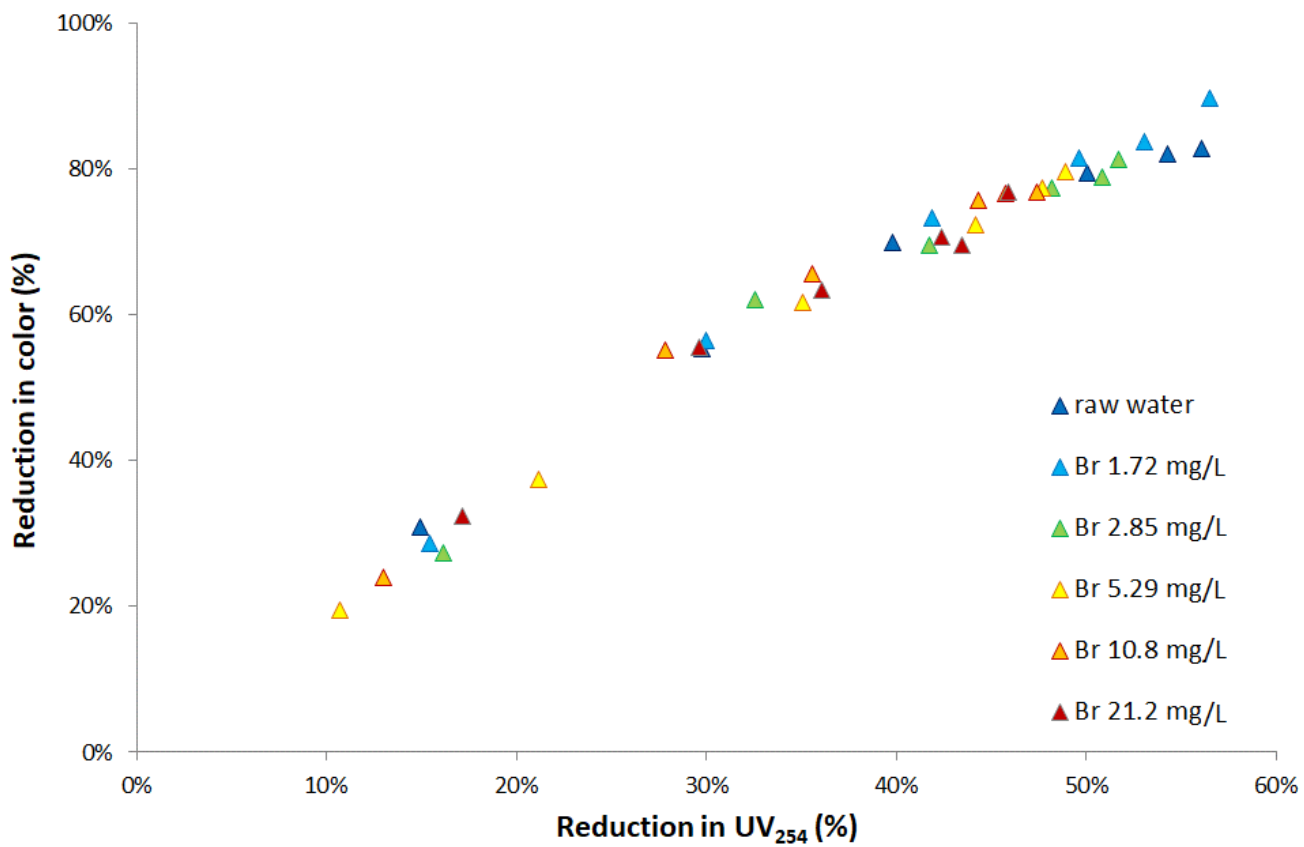
Figure 3. Relationship between changes of the color of ozonated wastewater and UVA$_{254}$ reduction
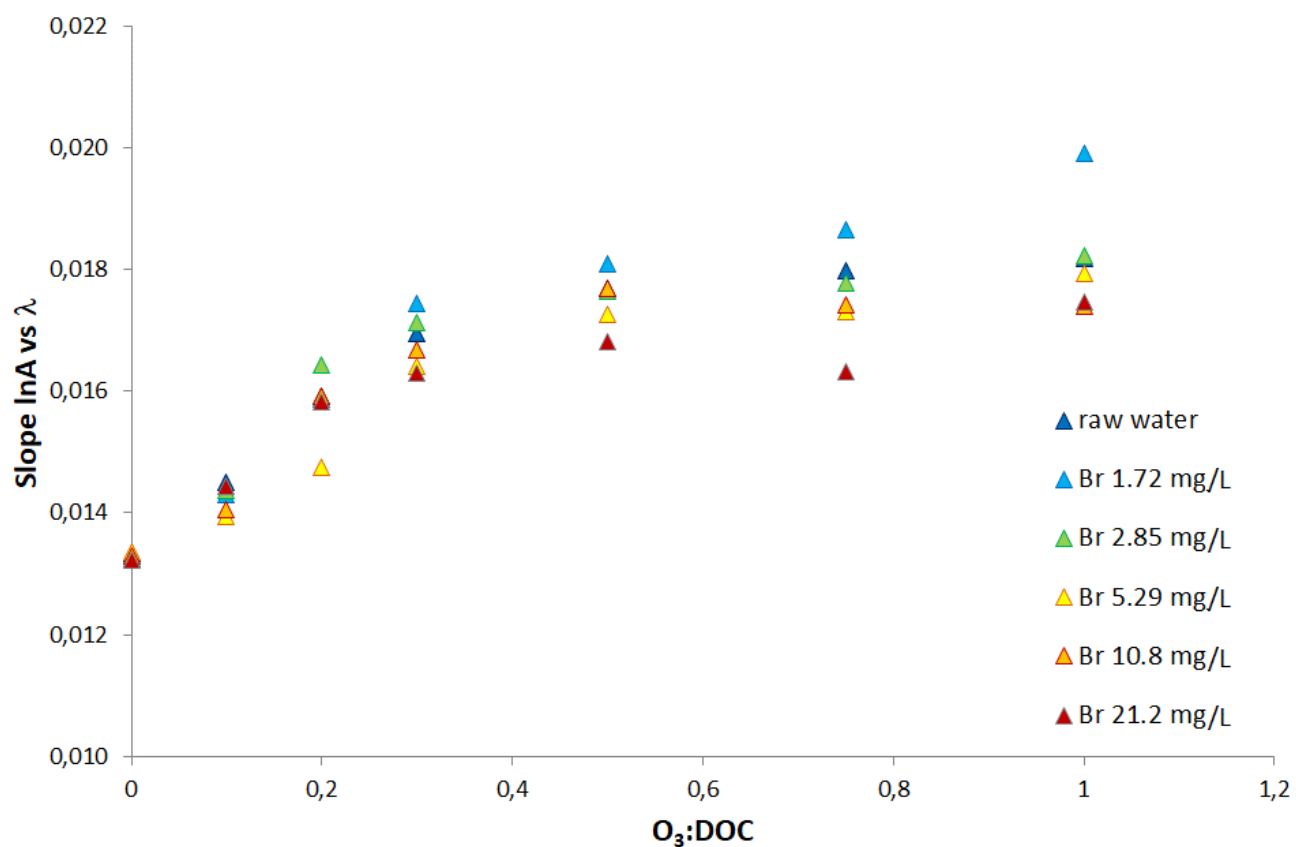
Figure 4. Effects of the specific ozone dose on the spectral slope of the absorbance of ozonated wastewater at varying bromide concentrations. The spectral slopes were determined for 300 to 400 nm wavelength range.

(a)
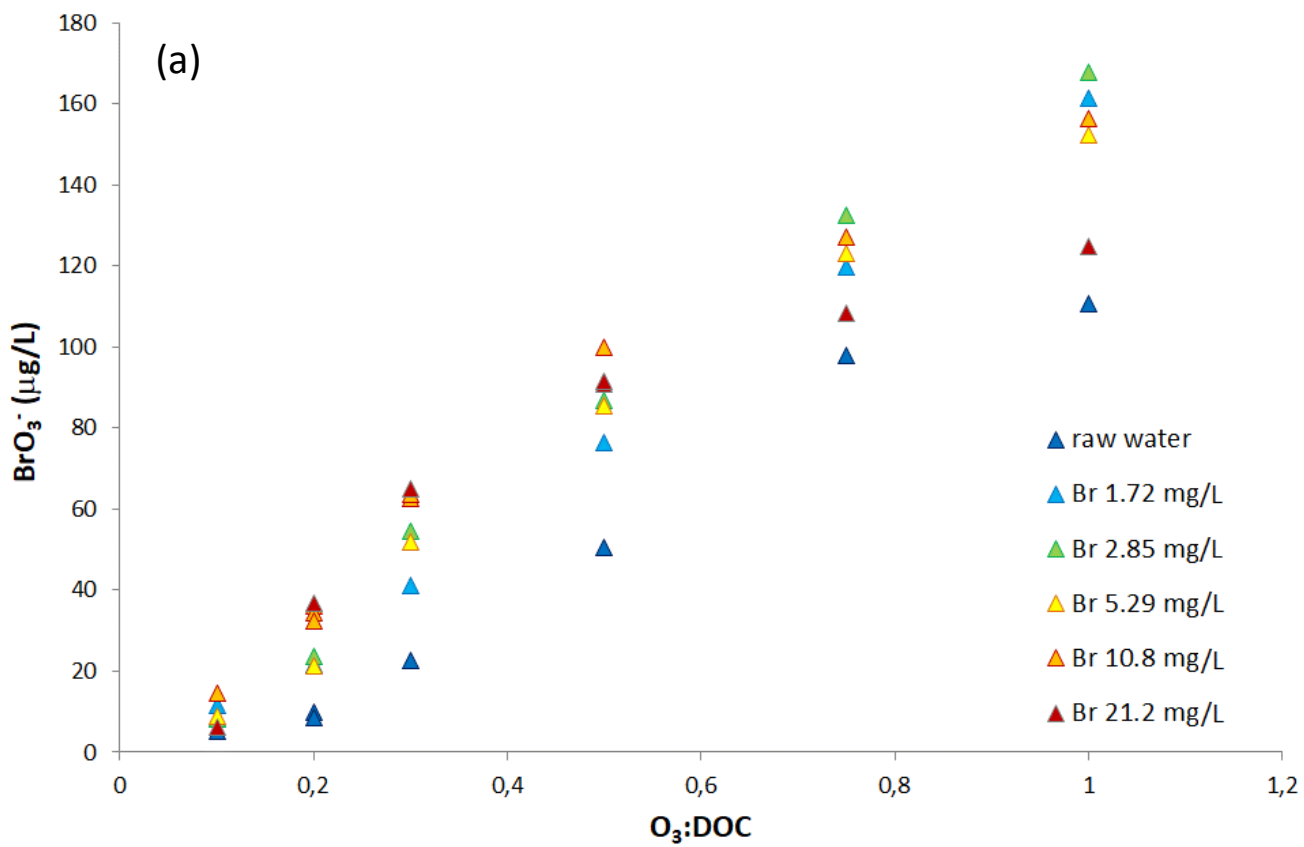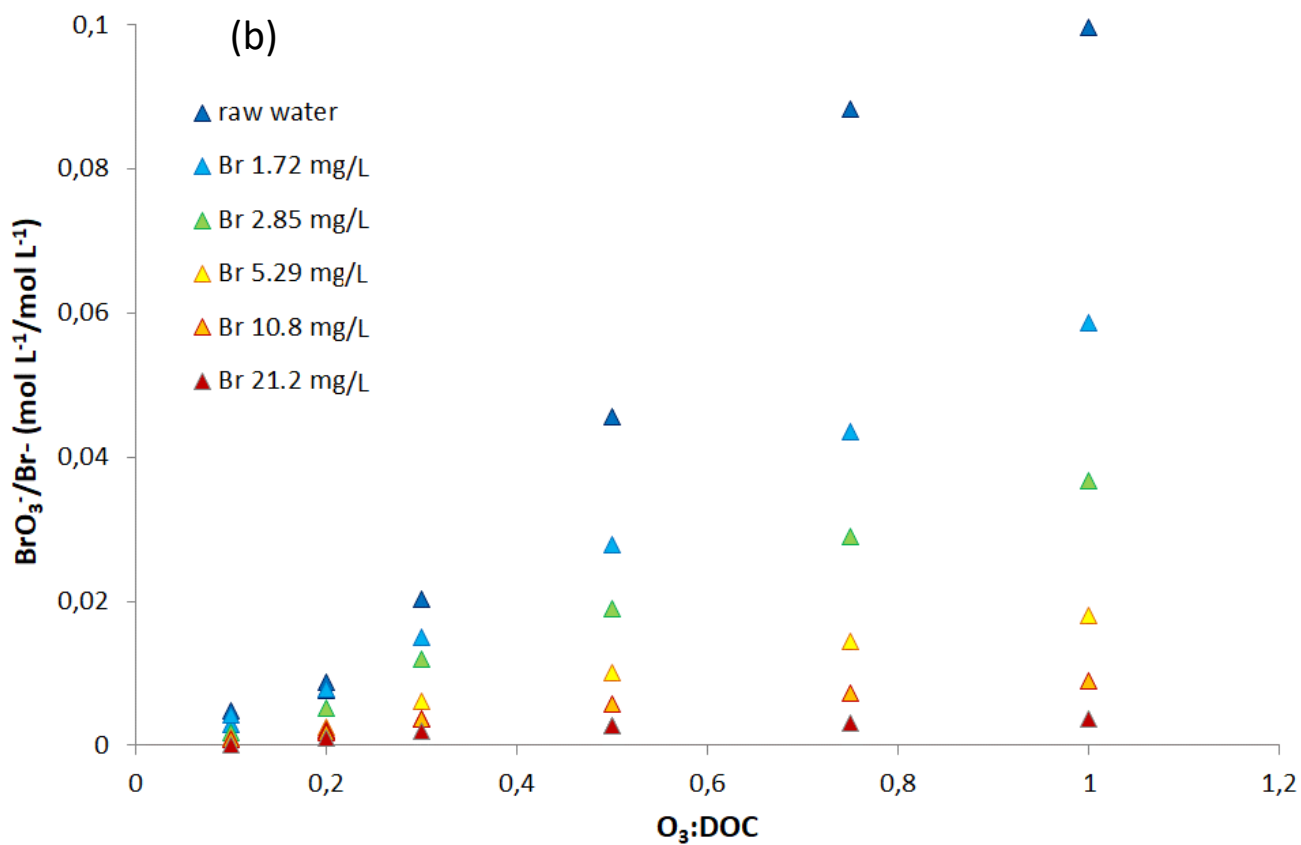
Figure 5. Relationships between bromate concentrations (a) and bromate molar yields (b) vs. specific ozone dose at varying bromide concentrations.

(a)

Legend:
- raw water
- Br 1.72 mg/L
- Br 2.85 mg/L
- Br 5.29 mg/L
- Br 10.8 mg/L
- Br 21.2 mg/L

Y-axis: BrO_3^- ($\mu g/L$)

X-axis: Reduction in UVA_{254}
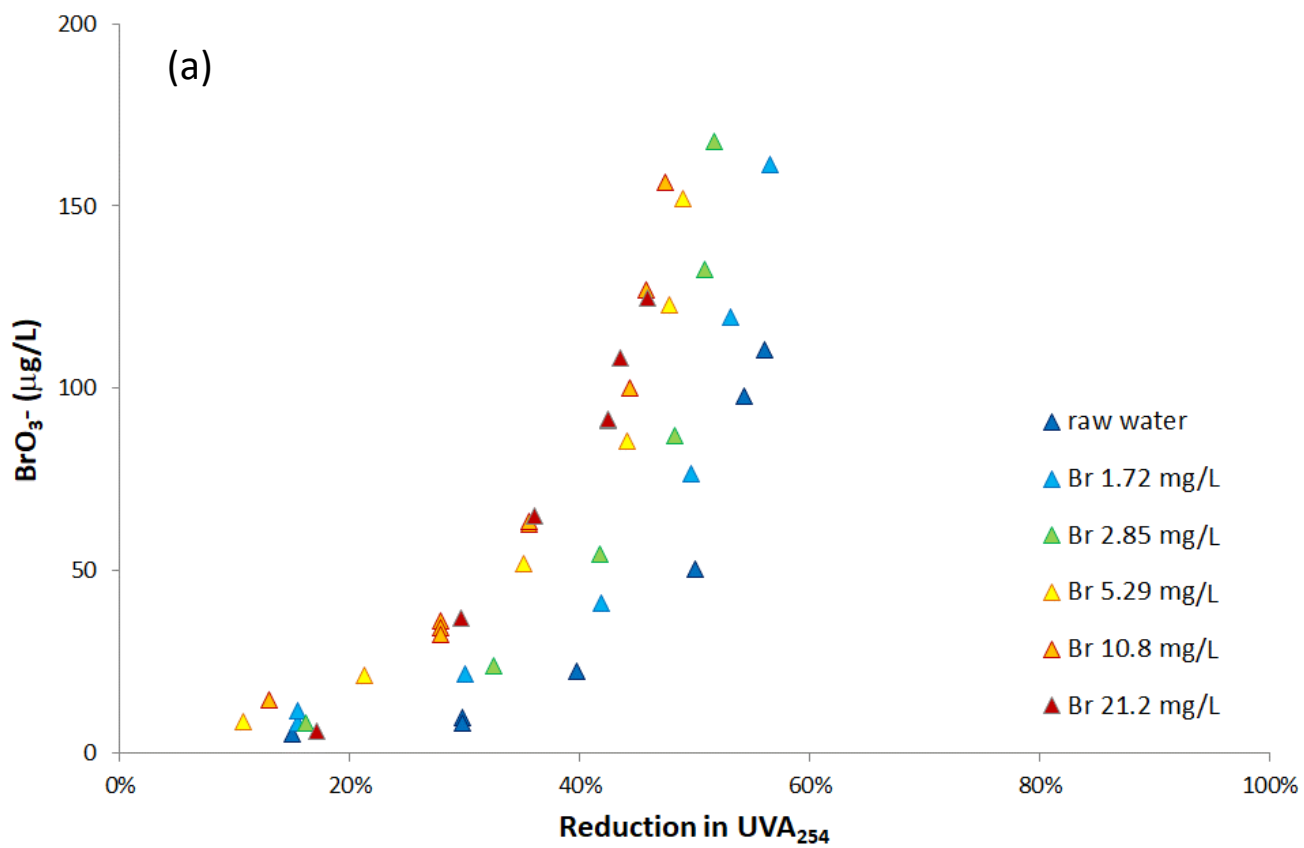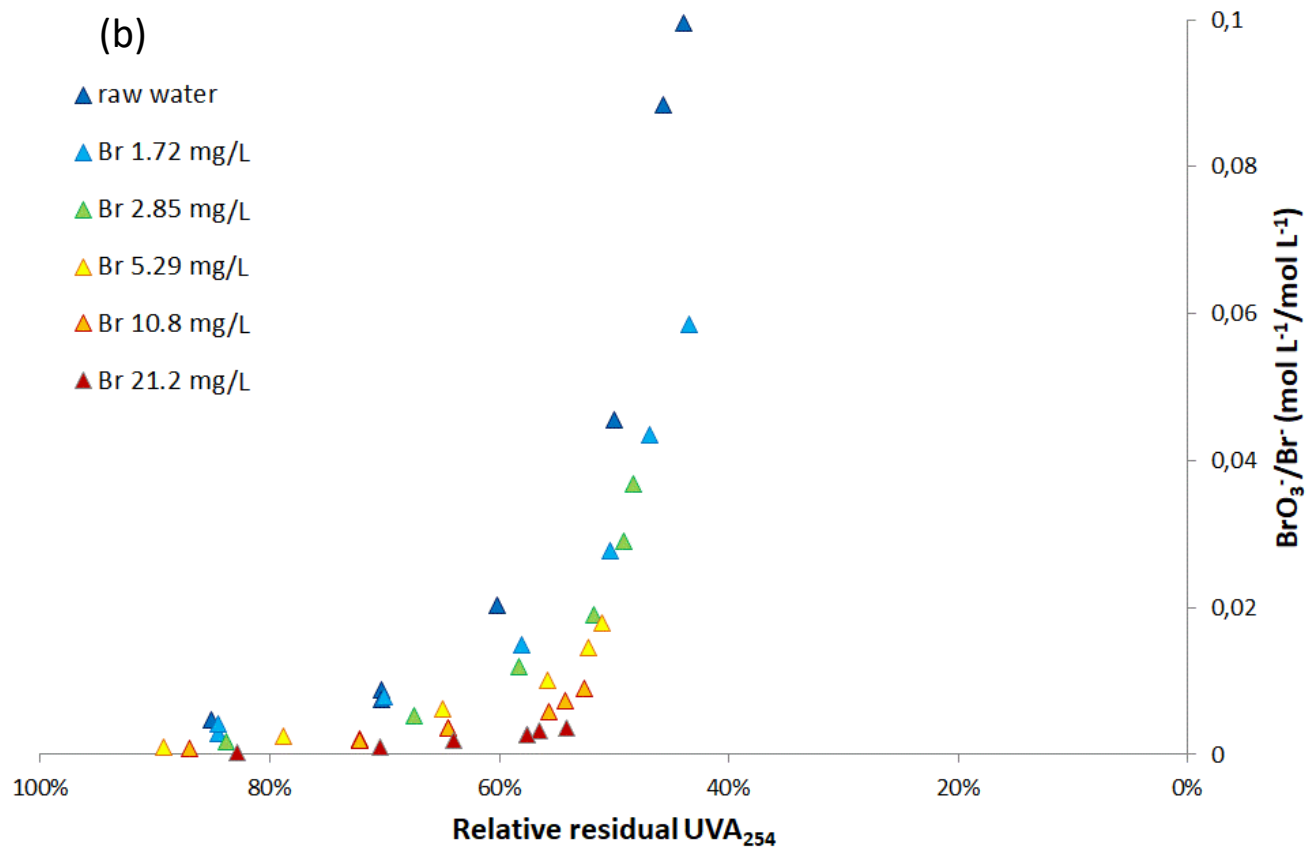
Figure 6. Relationships between bromate concentrations (a) and molar bromate yields (b) vs. decrease of UVA254
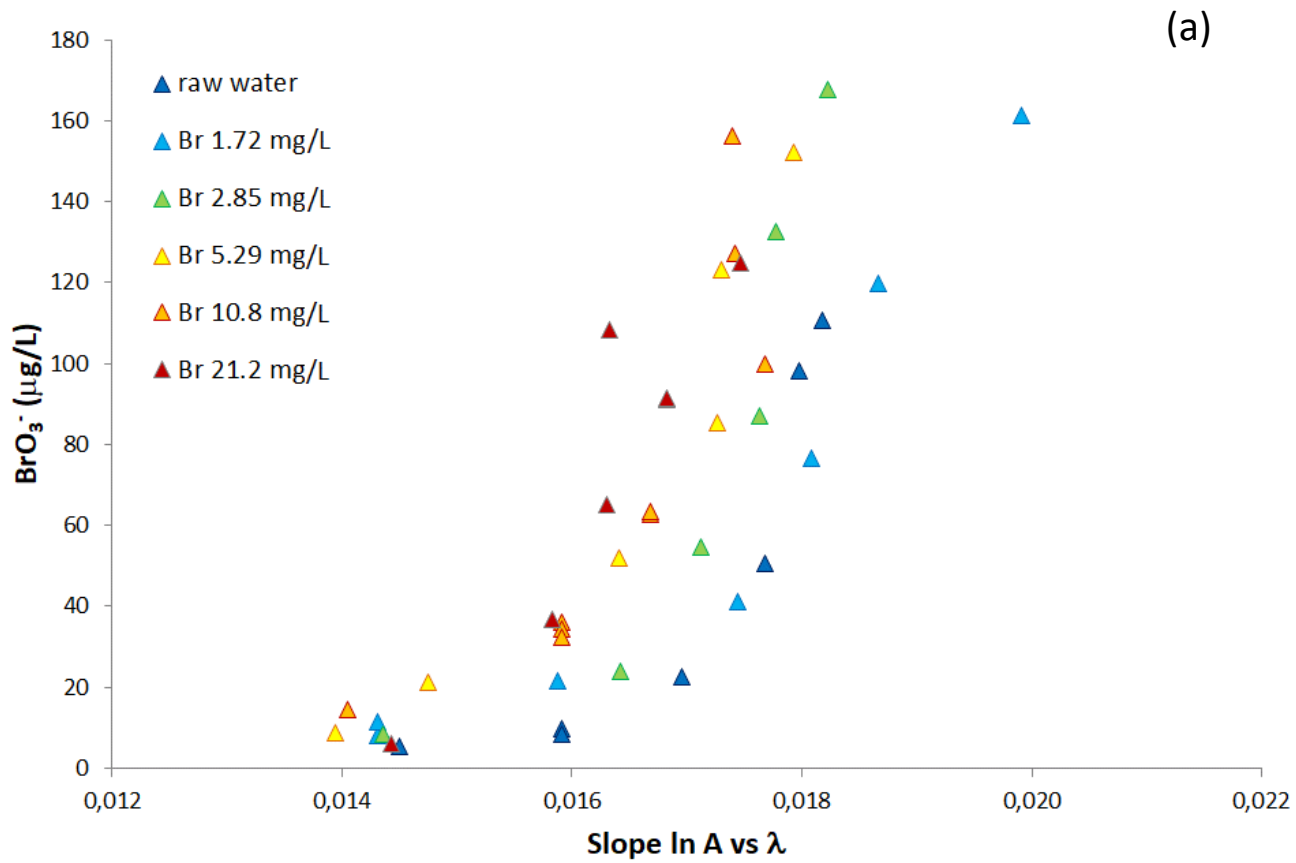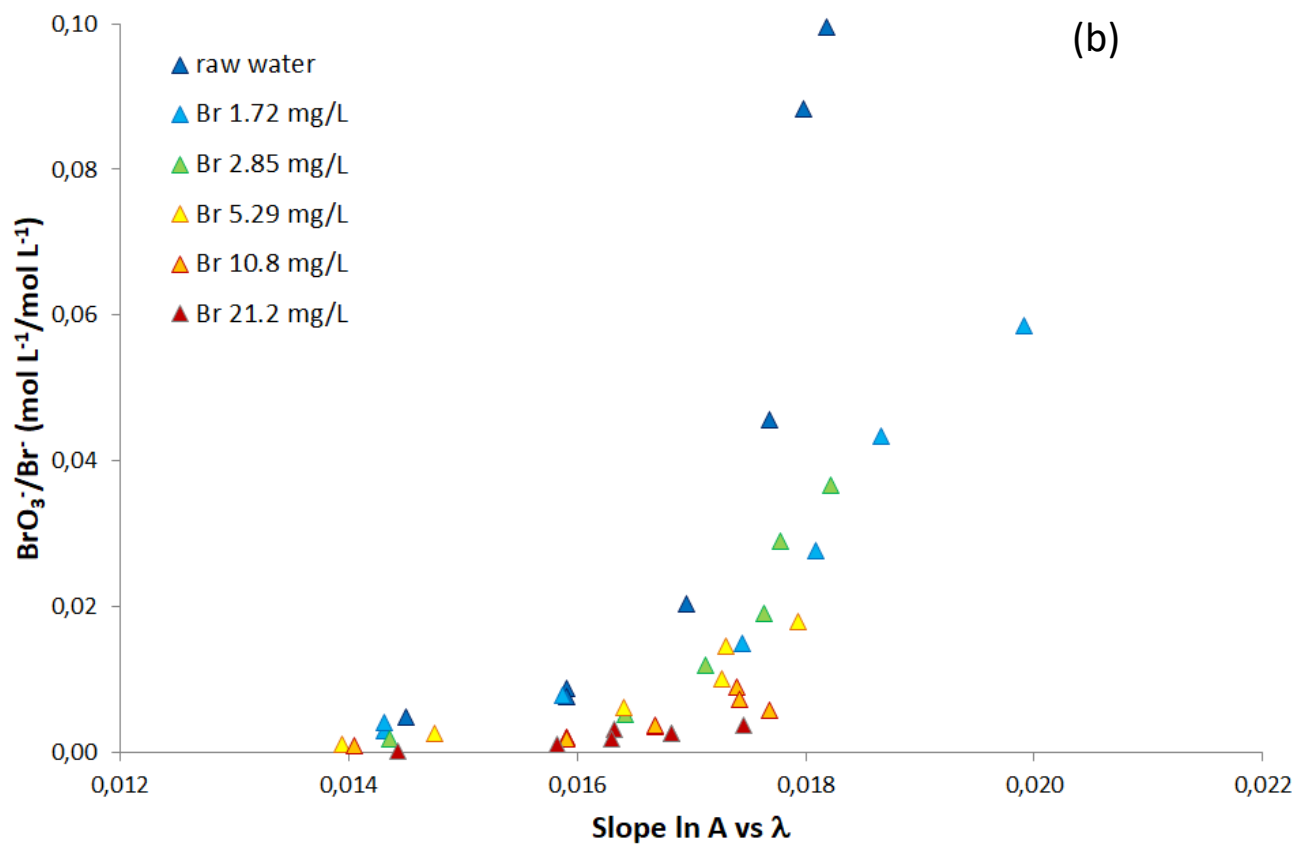
Figure 7. Relationships between bromate concentrations (a) and molar bromate yields (b) vs. changes of the spectral slope
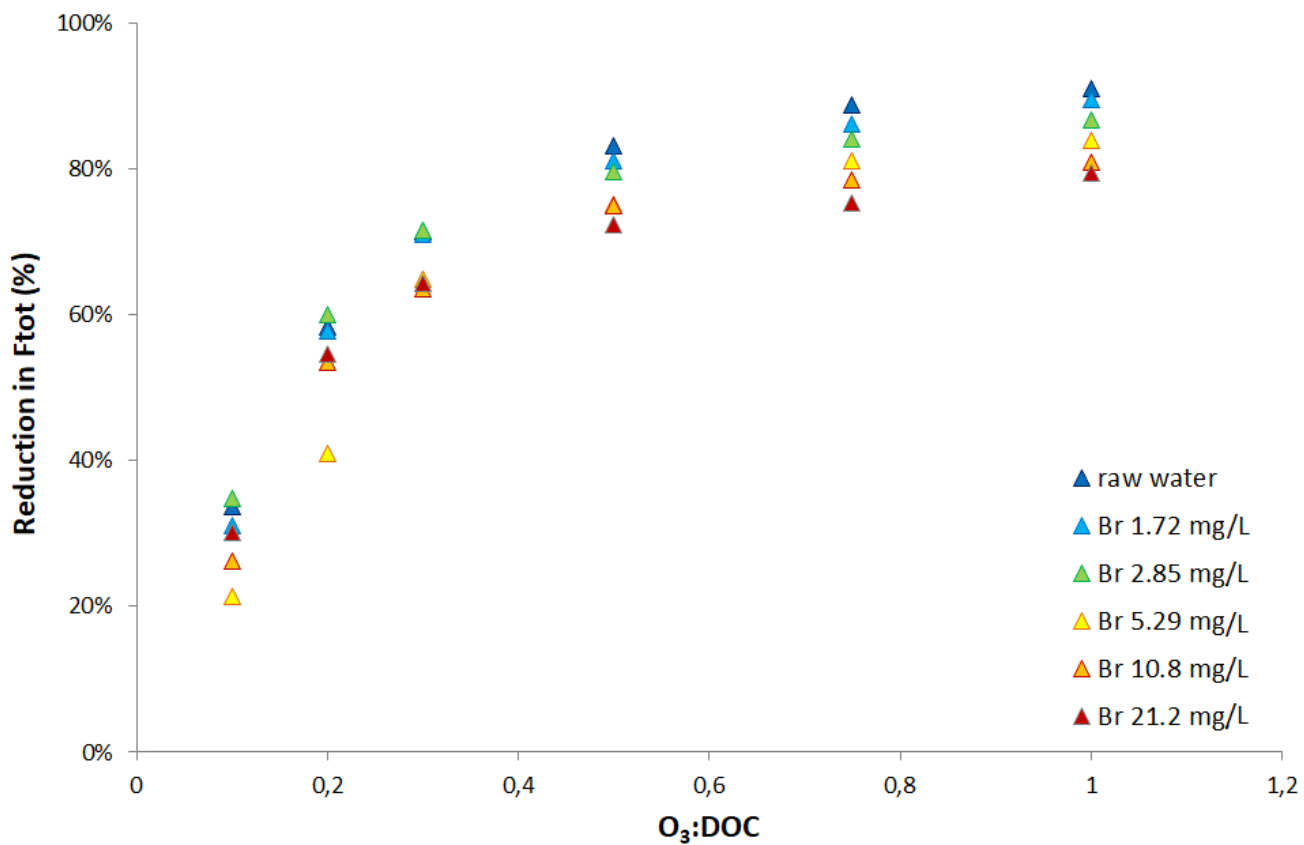
Figure 8. Relative reduction in total fluorescence of ozonated wastewater as a function of specific ozone doses and Br⁻ concentrations.
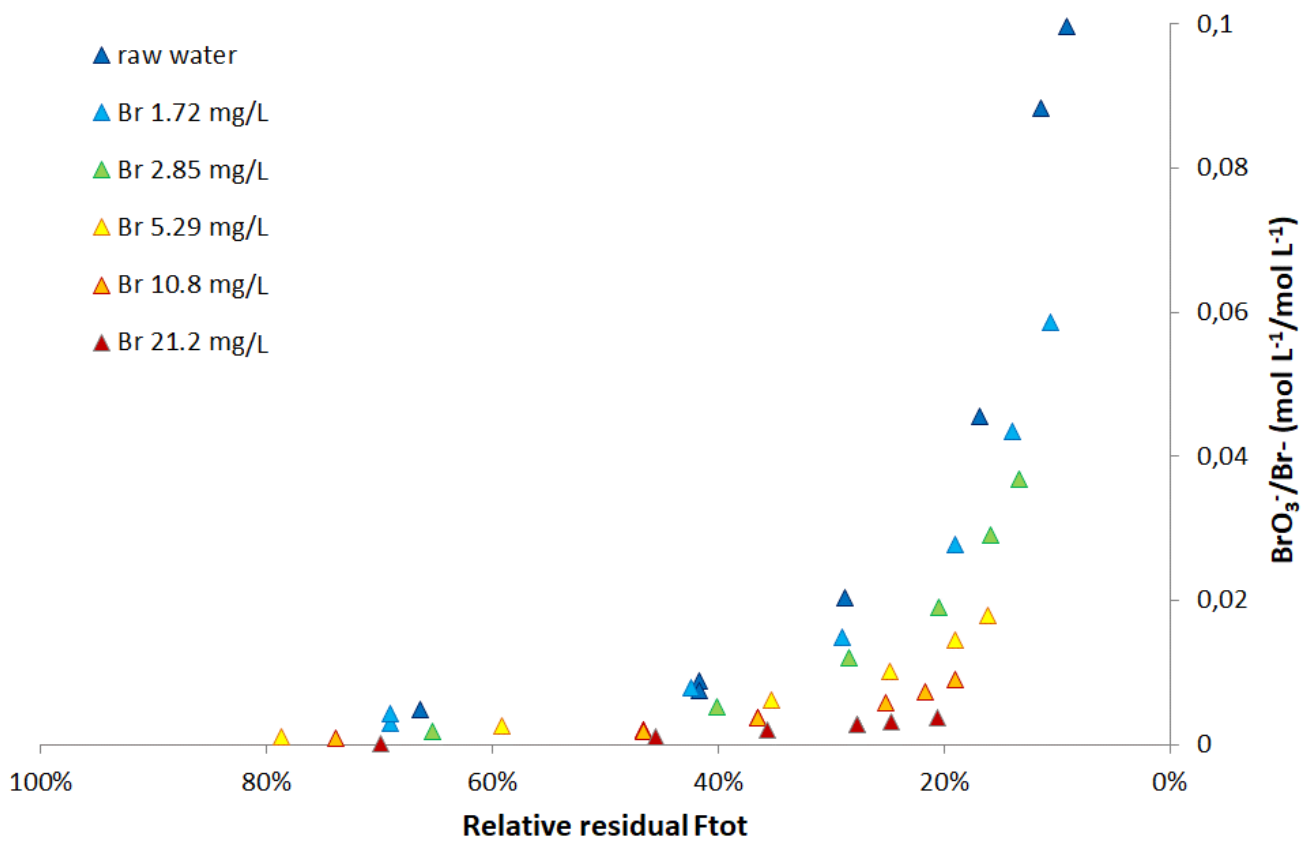
Figure 9. Molar bromate yields vs. the relative decrease of TF of ozonated wastewater.

Supplementary Material for

Use of Spectroscopic Indicators for the Prediction of Bromate Generation in Ozonated Wastewater Containing Variable Concentrations of Bromide

Barbara Ruffino[a,*], Gregory V. Korshin[b], Mariachiara Zanetti[a]

[a]Department of Environment, Land and Infrastructure Engineering, Politecnico di Torino, Torino, Italy

[b]Department of Civil and Environmental Engineering, University of Washington, Seattle, WA, USA

*Corresponding author
Barbara Ruffino
Department of Environment, Land and Infrastructure Engineering,
Politecnico di Torino,
Corso Duca degli Abruzzi 24, Torino, Italy
Ph. +39.011.0907663
Email: barbara.ruffino@polito.it

Table S1. Bromide concentrations (µg/L) in the water samples used in previous studies

Study	Br-, µg/L				
	Sample 1	Sample 2	Sample 3	Sample 4	Sample 5
Dickenson et al. (2009)	NA	-	-	-	-
Chon et al. (2015)	NA	58	86	39	-
Ross et al. (2016)	92	-	-	-	-
Li et al. (2017)	267.8	201.5	36.7	-	-
Wu et al. (2018)	58.4	12.1	11.0	NA	8.2

Procedure of sample preparation for batch tests

For the batch tests, 75 mL of filtered, raw wastewater were used. The volume of the raw wastewater was mixed with the volumes of ozone stock solution or deionized water detailed in Table S2 in order to simultaneously achieve the initial ozone concentration values of 0, 1, 2, 3, 5, 7.5 and 10 mg O_3/L and provide the same dilution ratio in all the samples. In all the samples the final volume was of 100 mL.

Table S2. Procedure of samples preparation for batch tests

Specific ozone dose, g O_3/g DOC	Raw water, mL	Deionized water, mL	Ozone stock solution, mL
0	75	25	0
0.1	75	22.5	2.5
0.2	75	20	5
0.3	75	17.5	7.5
0.5	75	12.5	12.5
0.75	75	6.25	18.75
1	75	0	25
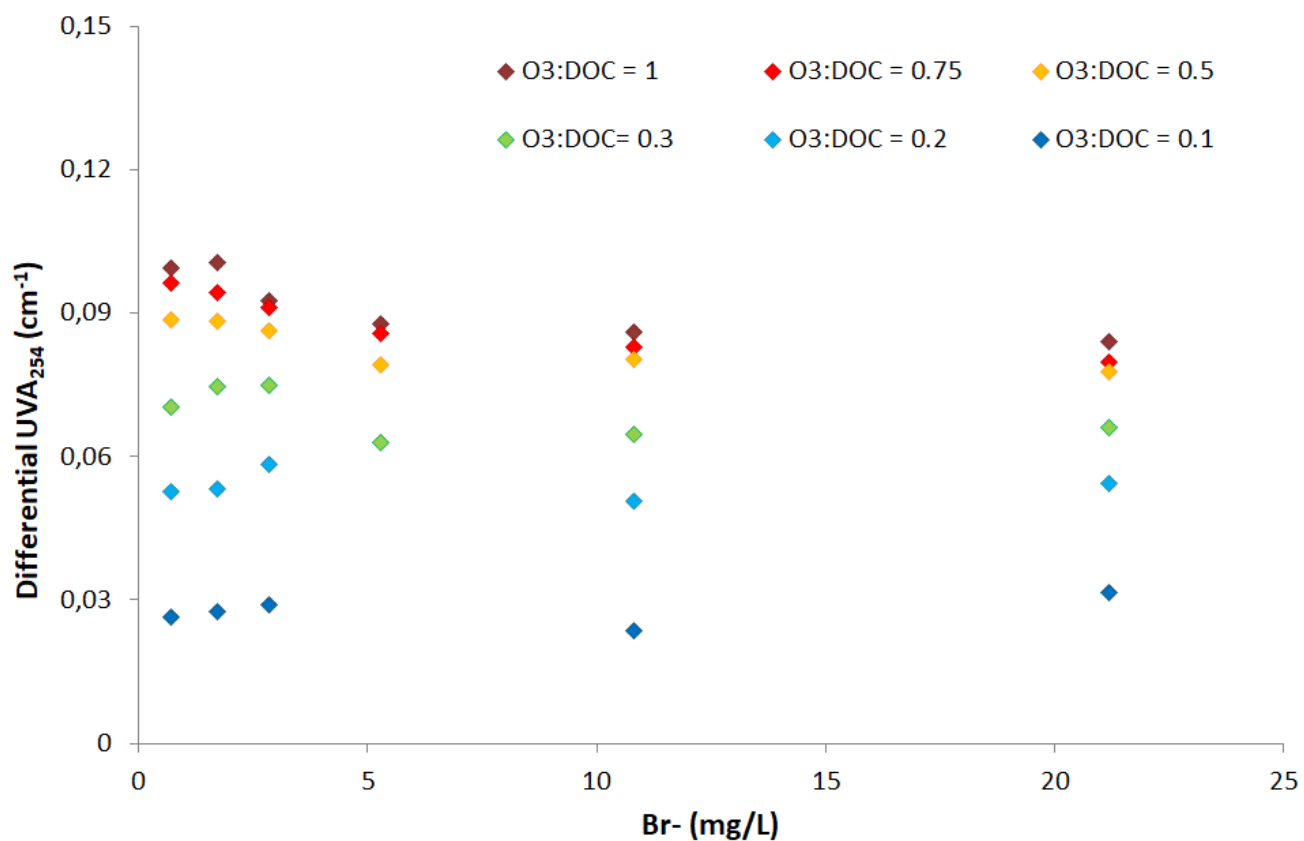
Figure S1. Changes in the differential UVA254 of the wastewater effluent as a function of bromide concentration for the ozone doses (0.1 – 1 mg O_3/ mg DOC) used in this study
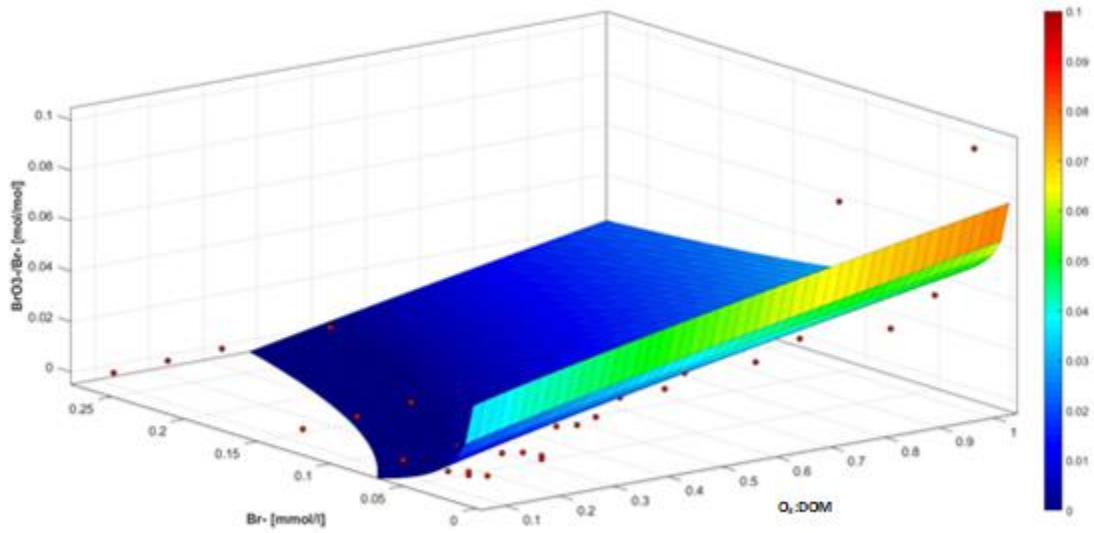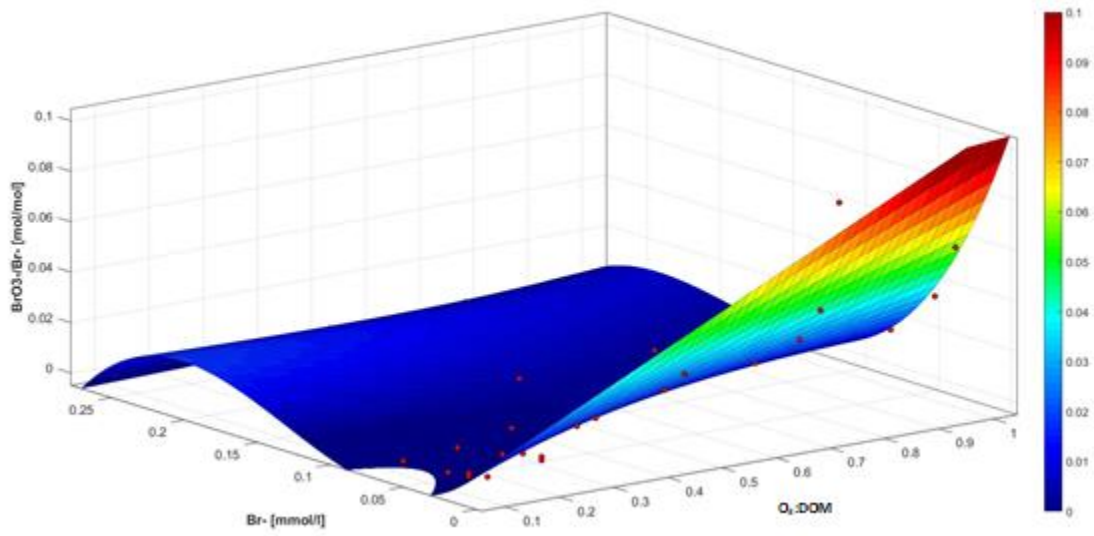
Figure S2. Bromate molar yield as a function of the specific ozone dose and bromide concentration. Experimental observations and exponential fit

The relation with an exponential form can be written as in Eq. (S1)

$$BrO_3\left(\frac{O_3}{DOC}, Br\right) = a + b\left(\frac{O_3}{DOC}\right)^n + c(Br)^m \qquad (S1)$$

With coefficients (with 95% confidence bounds):

a = 0.631 (-24.3, 25.56)

b = 0.04391 (0.01939, 0.06844

c = -0.6695 (-25.57, 24.23)

m = 0.01712 (-0.654, 0.6883)

n = 0.8684 (-0.3131, 2.05)

and a R^2 value of 0.665.

Figure S3. Bromate molar yield as a function of the specific ozone dose and bromide concentration. Experimental observations and third-order polynomial fit

The relation with a third-order polynomial form can be written as in Eq. (S2)

$$BrO_3\left(\frac{O_3}{DOC}, Br\right) = p_{00} + p_{10}\left(\frac{O_3}{DOC}\right) + p_{01}(Br) + p_{11}\left(\frac{O_3}{DOC}\right)(Br) + p_{02}(Br)^2 +$$

$$p_{12}\left(\frac{O_3}{DOC}\right)(Br)^2 + p_{03}(Br)^3 \qquad (S2)$$

With coefficients (with 95% confidence bounds):

p_{00} = 0.00248 (-0.006359, 0.01132)

p_{10} = 0.09967 (0.08598, 0.1134)
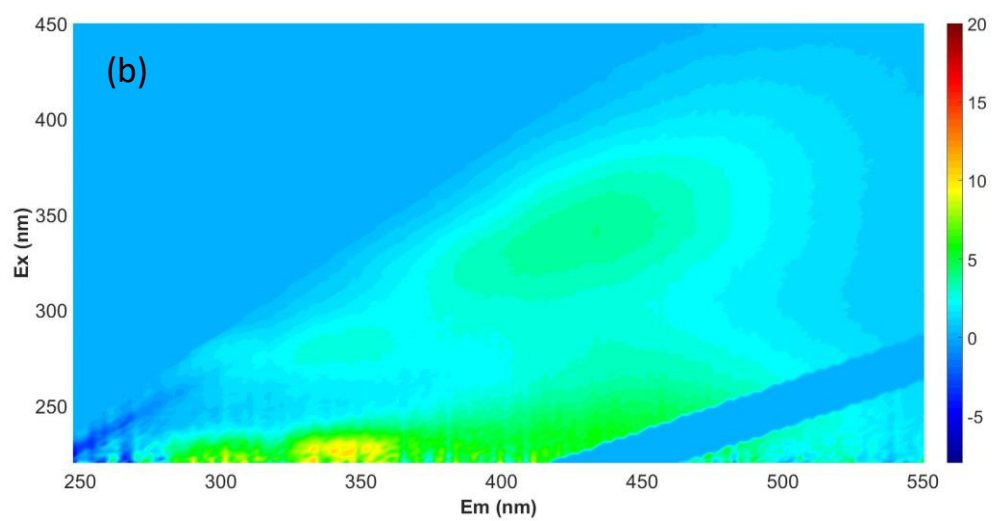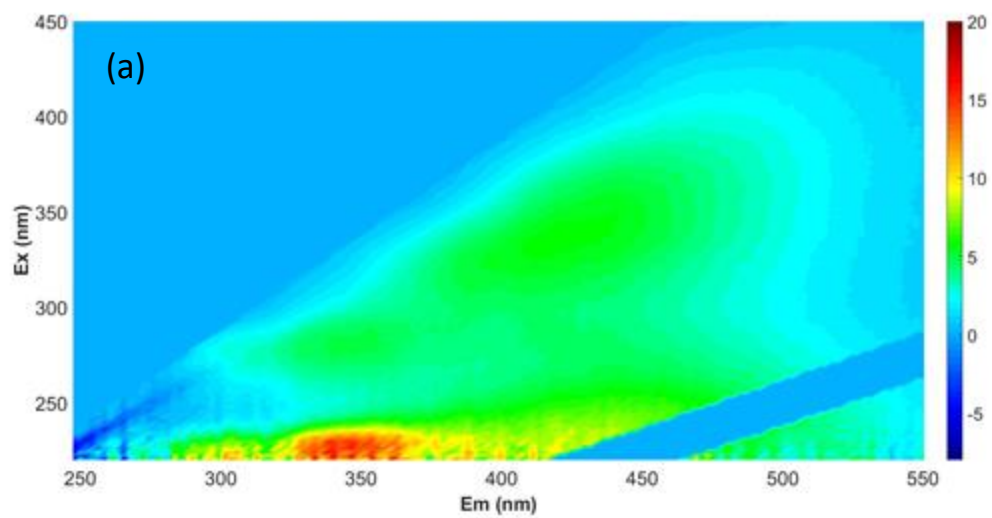
p_{01} = -0.5382 (-0.8887, -0.1876)

p_{11} = -1.24 (-1.558, -0.9218)

p_{02} = 6.575 (3.352, 9.797)

p_{12} = 3.363 (2.226, 4.501)

p_{03} = -17.34 (-25.17, -9.512)

and a R^2 value of 0.921.
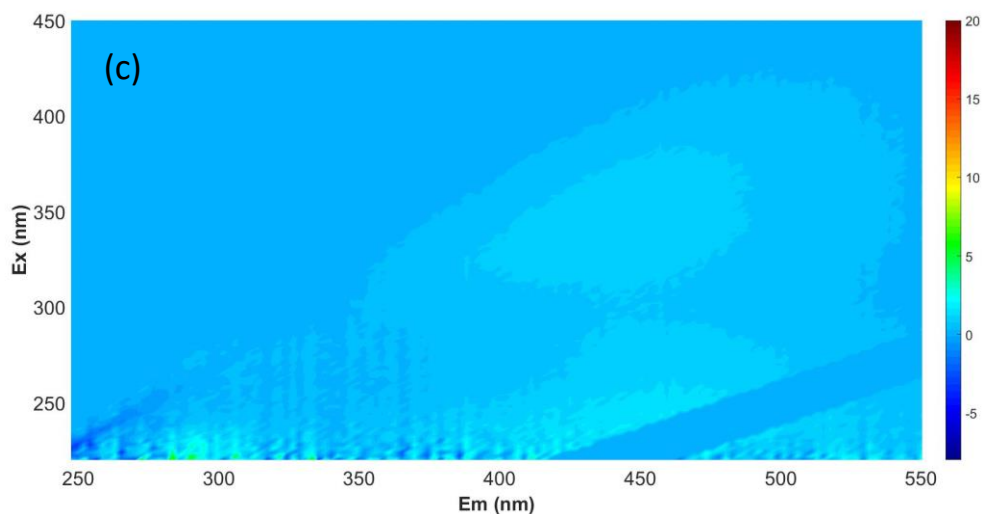
Figure S4. Fluorescence EEMs of the untreated raw sample (Br = 0.693 mg/L, a) and of the samples treated with 0.1 (b) and 0.5 (c) mg O_3/mg DOC

Fluorescence peaks in the range EM < 380 nm are due to substances containing a single aromatic structure to which amino groups are attached. These structures are typical of proteins or soluble microbial products (SMPs). Conversely, fluorescence peaks characterized by EM > 380 nm are due to the presence of substances containing polycyclic aromatic structures. Peaks in the low excitation range (240-300 nm) are deemed to be indicative of the presence of fulvic-like compounds and peaks in the high excitation range (300-420 nm) of humic-like species.
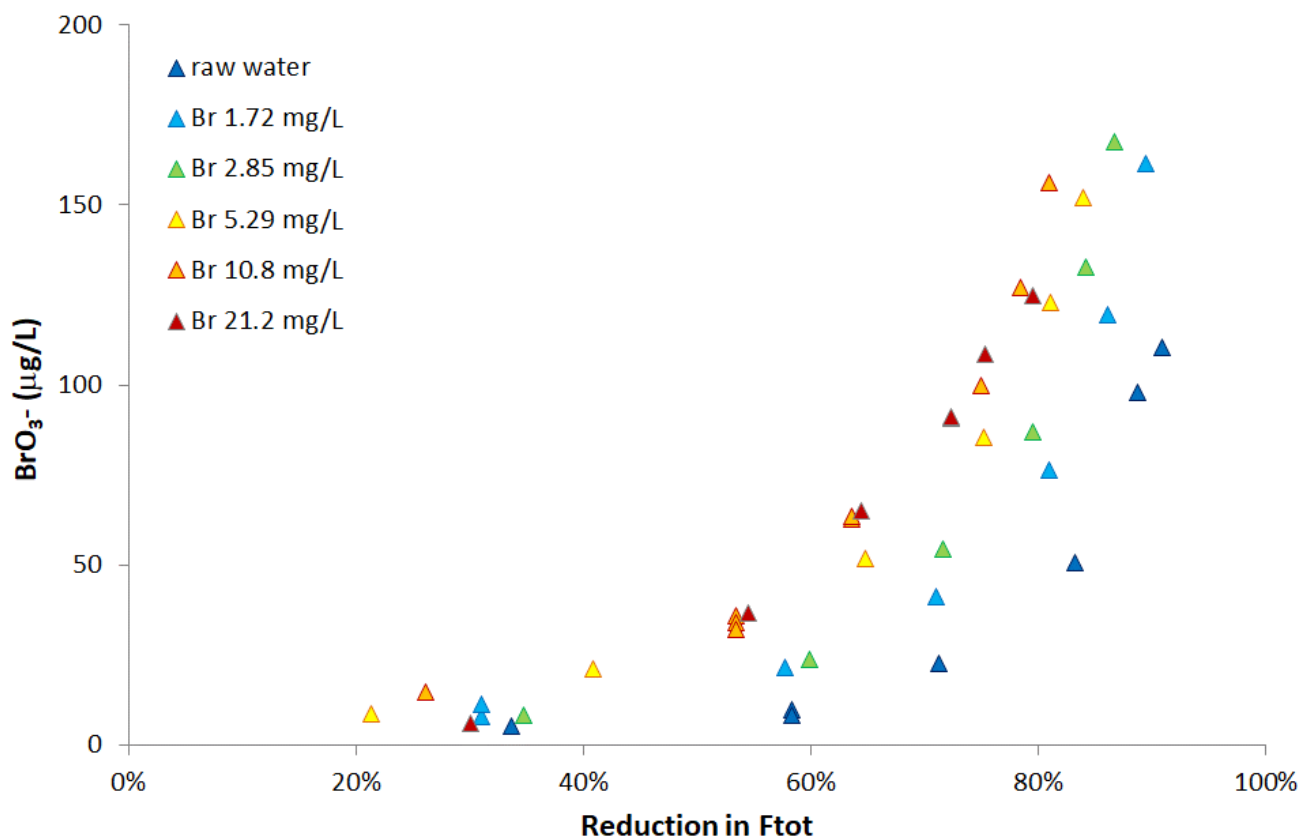
Figure S5. Generation of bromate as a function of the reduction of TF